
InfoBridge: Mutual Information estimation via Bridge Matching

Sergei Kholkin¹ Ivan Butakov^{1,2} Evgeny Burnaev^{1,3} Nikita Gushchin¹ Alexander Korotin^{1,3}

Abstract

Diffusion bridge models have recently become a powerful tool in the field of generative modeling. In this work, we leverage their power to address another important problem in machine learning and information theory – the estimation of the mutual information (MI) between two random variables. We show that by using the theory of diffusion bridges, one can construct an unbiased estimator for data posing difficulties for conventional MI estimators. We showcase the performance of our estimator on a series of standard MI estimation benchmarks.

1. Introduction

Information theory offers an extensive set of tools for quantifying probabilistic relations between random variables. It is widely used in machine learning for advanced statistical analysis (Berrett & Samworth, 2017; Sen et al., 2017; Duong & Nguyen, 2023b; Bounoua et al., 2024a), assessment of deep neural networks’ performance and generalization capabilities (Tishby & Zaslavsky, 2015; Xu & Raginsky, 2017; Goldfeld et al., 2019; Steinke & Zakyntinou, 2020; Amjad et al., 2022; Butakov et al., 2024b), self-supervised and semi-supervised learning (Linsker, 1988; Bell & Sejnowski, 1995; Hjelm et al., 2019; Stratos, 2019; Bachman et al., 2019; Veličković et al., 2019; van den Oord et al., 2019; Tschannen et al., 2020) and regularization or alignment in generative modeling (Chen et al., 2016; Belghazi et al., 2018; Ardizzone et al., 2020; Wang et al., 2024).

The majority of the aforementioned applications revolve around one of the central information-theoretic quantities – *mutual information* (MI). Due to several outstanding properties, MI is widely used as an invariant measure of non-linear dependence between random variables. Unfortunately, recent studies suggest that the curse of dimensionality is

highly pronounced when estimating MI (Goldfeld et al., 2020; McAllester & Stratos, 2020). Additionally, it is argued that long tails, high values of MI and some other particular features of complex probability distributions can make mutual information estimation even more challenging (Czyż et al., 2023). On the other hand, recent developments in neural estimation methods demonstrate that sophisticated parametric estimators can achieve notable practical success in situations where traditional mutual information estimation techniques struggle (Belghazi et al., 2018; van den Oord et al., 2019; Song & Ermon, 2020; Rhodes et al., 2020; Ao & Li, 2022; Butakov et al., 2024a). Among neural estimators, generative approaches are of particular interest, as they have proven to be effective in handling complex data (Duong & Nguyen, 2023a; Franzese et al., 2024; Butakov et al., 2024a). Since MI estimation is closely tied to approximation of a joint probability distribution, one can argue that leveraging state-of-the-art generative models, e.g., diffusion models, may result in additional performance gains.

Diffusion Bridge Matching. Diffusion models are a powerful type of generative models that show an impressive quality of image generation (Ho et al., 2020; Rombach et al., 2022). However, they have some disadvantages, such as the inability to perform data-to-data translation via diffusion. To tackle this problem, a novel promising approach based on a Reciprocal Processes (Léonard et al., 2014) and Schrödinger Bridges theory (Schrödinger, 1932; Léonard, 2013) have risen. This approach is called the *diffusion bridge matching* and is used for learning generative models as diffusion processes for data-to-data translation. This type of models has shown itself as a powerful approach for numerous applications in biology (Tong et al., 2024; Bunne et al., 2023), chemistry (Somnath et al., 2023; Igashov et al., 2024), computer vision (Liu et al., 2023; Shi et al., 2023; Zhou et al., 2024), speech processing (Chen et al., 2023) and unpaired learning (Gushchin et al., 2024b;a; Shi et al., 2023).

Contributions. In this work, we employ the Diffusion Bridge Matching to tackle the problem of MI estimation.

- Theory.** We propose an unbiased mutual information estimator based on reciprocal processes, their diffusion representations and the Girsanov theorem (§4.1).

¹Skolkovo Institute of Science and Technology ²Moscow Institute of Physics and Technology ³Artificial Intelligence Research Institute. Correspondence to: Sergei Kholkin <s.kholkin@skoltech.ru>, Alexander Korotin <a.korotin@skoltech.ru>.

2. **Practice.** Building on the proposed theoretical framework and the powerful generative methodology of diffusion bridges, we develop a practical algorithm for MI estimation, named *InfoBridge* (§4.3). We demonstrate that our method achieves performance comparable to existing approaches on low-dimensional benchmarks and either comparable or superior performance on image data benchmarks (§5).

Notations. We work in \mathbb{R}^D , which is the D -dimensional Euclidean space equipped with the Euclidean norm $\|\cdot\|$. We use $\mathcal{P}(\mathbb{R}^D)$ to denote the absolutely continuous Borel probability distributions whose variance and differential entropy are finite. To denote the density of $q \in \mathcal{P}(\mathbb{R}^D)$ at a point $x \in \mathbb{R}^D$, we use $q(x)$. We write $\text{KL}(\cdot\|\cdot)$ to denote the Kullback-Leibler divergence between two distributions. In turn, $H(\cdot)$ denotes the differential entropy of a distribution. We use Ω to denote the space of trajectories, i.e., continuous \mathbb{R}^D -valued functions of $t \in [0, 1]$. We write $\mathcal{P}(\Omega)$ to denote the probability distributions on the trajectories Ω whose marginals at $t = 0$ and $t = 1$ belong to $\mathcal{P}(\mathbb{R}^D)$; this is the set of stochastic processes. We use dW_t to denote the differential of the standard Wiener process $W \in \mathcal{P}(\Omega)$. We use $Q_{|x_0}$ and $Q_{|x_0, x_1}$ to denote the distribution of stochastic process Q conditioned on Q 's values x_0 and x_0, x_1 at times $t = 0$ and $t = 0, 1$, respectively. For a process $Q \in \mathcal{P}(\Omega)$, we denote its marginal distribution at time t by $q(x_t) \in \mathcal{P}(\mathbb{R}^D)$, and if process conditioned on its value x_s at time s , the marginal distribution of such a process at time t would be denoted as $q(x_t|x_s) \in \mathcal{P}(\mathbb{R}^D)$.

2. Background

Mutual information. Information theory is a well-established framework for analyzing and quantifying interactions between random vectors. In this framework, mutual information (MI) serves as a fundamental and invariant measure of the non-linear dependence between two \mathbb{R}^D -valued random vectors X_0, X_1 . It is defined as follows:

$$I(X_0; X_1) = \text{KL}(\Pi_{X_0, X_1} \|\Pi_{X_0} \otimes \Pi_{X_1}), \quad (1)$$

where Π_{X_0, X_1} and Π_{X_0}, Π_{X_1} are the joint and marginal distributions of a pair of random vectors (X_0, X_1) . If the corresponding PDF $\pi(x_0, x_1)$ exists, the following also holds:

$$I(X_0; X_1) = \mathbb{E}_{x_0, x_1 \sim \pi(x_0, x_1)} \log \frac{\pi(x_0, x_1)}{\pi(x_0)\pi(x_1)}. \quad (2)$$

Mutual information is symmetric, non-negative and equals zero if and only if X_0 and X_1 are independent. MI is also invariant to bijective mappings: $I(X_0; X_1) = I(g(X_0); X_1)$ if g^{-1} exists and g, g^{-1} are measurable (Cover & Thomas, 2006; Polyanskiy & Wu, 2024).

Brownian Bridge. Let W^ϵ be the Wiener process with a constant volatility ϵ , i.e., it is described by the SDE $dW^\epsilon = \sqrt{\epsilon}dW_t$, where W_t is the standard Wiener process. Let $W_{|x_0, x_1}^\epsilon$ denote the process W^ϵ conditioned its on values x_0, x_1 at times $t = 0, 1$, respectively. This process $W_{|x_0, x_1}^\epsilon$ is called the Brownian Bridge (Ibe, 2013, Chapter 9).

Reciprocal processes. Reciprocal processes are a class of stochastic processes that have recently gained attention of research community in the contexts of stochastic optimal control (Léonard et al., 2014), Schrödinger Bridges (Schrödinger, 1932; Léonard, 2013), and diffusion generative modeling (Liu et al., 2023; Gushchin et al., 2024a). In our paper, we consider a *particular case* of reciprocal processes which are induced by the Brownian Bridge $W_{|x_0, x_1}^\epsilon$.

Consider a joint distribution $\pi(x_0, x_1) \in \mathcal{P}(\mathbb{R}^{D \times 2})$ and define the process $Q_\pi \in \mathcal{P}(\Omega)$ as a mixture of Brownian bridges $W_{|x_0, x_1}^\epsilon$ with weights $\pi(x_0, x_1)$:

$$Q_\pi \stackrel{\text{def}}{=} \int W_{|x_0, x_1}^\epsilon d\pi(x_0, x_1).$$

This implies that to get trajectories of Q_π one has to first sample the start and end points, x_0 and x_1 , at times $t = 0$ and $t = 1$ from $\pi(x_0, x_1)$ and then simulate the Brownian Bridge $W_{|x_0, x_1}^\epsilon$. Due to the non-causal nature of trajectory formation, such a process is, in general, non markovian. The set of all mixtures of Brownian Bridges can be described as:

$$\{Q \in \mathcal{P}(\Omega) \text{ s.t. } \exists \pi \in \mathcal{P}(\mathbb{R}^{D \times 2}) : Q = Q_\pi\}$$

and is called the set of *reciprocal processes* (for W^ϵ).

Reciprocal processes conditioned on the point. Consider a reciprocal process Q_π conditioned on some start point x_0 . Let the resulting processes be denoted as $Q_{\pi|x_0}$, which remains reciprocal. Then, if some regularity assumptions are met (Shi et al., 2023, Appx C.1) process $Q_{\pi|x_0}$ is known as the Schrödinger Föllmer process (Huang et al., 2024; Vargas et al., 2023). While Q_π itself is, in general, not markovian, $Q_{\pi|x_0}$ **is markovian**. Furthermore, it is a diffusion process governed by the following SDE:

$$Q_{\pi|x_0} : dx_t = v_{x_0}(x_t, t)dt + \sqrt{\epsilon}dW_t, x_0 \sim \delta(x_0),$$

$$v_{x_0}(x_t, t) = \mathbb{E}_{x_1 \sim q_\pi(x_1|x_t, x_0)} \left[\frac{x_1 - x_t}{1 - t} \right]. \quad (3)$$

Representations of reciprocal processes. The process Q_π can be naturally represented as a mixture of processes $Q_{\pi|x_0}$ conditioned on the starting points x_0 :

$$Q_\pi = \int Q_{\pi|x_0} d\pi(x_0).$$

Therefore, one may also express Q_π via an SDE but with, in general, non-markovian drift (conditioned on x_0):

$$Q_\pi : dx_t = v(x_t, t, x_0)dt + \sqrt{\epsilon}dW_t, x_0 \sim \pi(x_0),$$

$$v(x_t, t, x_0) = v_{x_0}(x_t, t) = \mathbb{E}_{x_1 \sim q_\pi(x_1|x_t, x_0)} \left[\frac{x_1 - x_t}{1 - t} \right]. \quad (4)$$

Conditional Bridge Matching. Although the drift $v_{x_0}(x_t, t)$ of Q_π in (3) admits a closed form, it usually cannot be computed or estimated directly due to the unavailability of a way to easily sample from $\pi(x_1|x_t, x_0)$. However, it can be recovered by solving the following regression problem:

$$v_{x_0} = \arg \min_u \mathbb{E}_{x_1 \sim q_\pi(x_1, x_t|x_0)} \left\| \frac{x_1 - x_t}{1 - t} - u(x_t, t) \right\|^2, \quad (5)$$

which optimizes over drifts $u : \mathbb{R}^D \times [0, 1] \rightarrow \mathbb{R}^D$. The same holds for the Q_π and its drift $v(x_t, t, x_0)$ through the addition of expectation w.r.t. $\pi(x_0)$:

$$v = \arg \min_u \mathbb{E}_{q_\pi(x_1, x_t|x_0)\pi(x_0)} \left\| \frac{x_1 - x_t}{1 - t} - u(x_t, t, x_0) \right\|^2 =$$

$$= \arg \min_u \mathbb{E}_{q_\pi(x_1, x_t, x_0)} \left\| \frac{x_1 - x_t}{1 - t} - u(x_t, t, x_0) \right\|^2, \quad (6)$$

where $u : \mathbb{R}^D \times [0, 1] \times \mathbb{R}^D \rightarrow \mathbb{R}^D$. Problem (6) is usually solved with standard deep learning techniques. Namely, one parametrizes u with a neural network v_θ , and minimizes (6) using stochastic gradient descent and samples drawn from $q_\pi(x_0, x_t, x_1)$. The latter sampling is easy if one can sample from $\pi(x_0, x_1)$. Indeed, $q_\pi(x_0, x_t, x_1) = q_\pi(x_t|x_0, x_1)\pi(x_0, x_1)$, and one can sample first from $\pi(x_0, x_1)$ and then from $q_\pi(x_t|x_0, x_1)$, which is just the Brownian Bridge.

Such a procedure of learning drift v with a neural network is popular in generative modeling to solve a problem of sampling from conditional distribution $\pi(x_1|x_0)$ and is frequently applied in the image-to-image transfer (Liu et al., 2023). The procedure of learning drift $v(x_t, t, x_0)$ (6) is usually called the *conditional* (or augmented) *bridge matching* (De Bortoli et al., 2023; Zhou et al., 2024). In addition, such procedure can also be derived through the well-celebrated Doob h -transform (De Bortoli et al., 2023; Zhou et al., 2024; Palmowski & Rolski, 2002) or reversing a diffusion (Zhou et al., 2024).

KL divergence between diffusion processes. Consider two diffusion processes with the same volatility coefficient $\sqrt{\epsilon}$ that start at the same distribution π_0 :

$$Q^A : dx_t = f^A(x_t, t)dt + \sqrt{\epsilon}dW_t, x_0 \sim \pi_0$$

$$Q^B : dx_t = f^B(x_t, t)dt + \sqrt{\epsilon}dW_t, x_0 \sim \pi_0$$

By the application of the disintegration theorem (Léonard, 2014, §1) and the Girsanov theorem (Øksendal, 2003, §8.6) one can derive the KL divergence between these diffusions:

$$\text{KL}(Q^A \| Q^B) =$$

$$= \frac{1}{2\epsilon} \int_0^1 \mathbb{E}_{x_t \sim q^A(x_t)} [\|f^A(x_t, t) - f^B(x_t, t)\|_2^2] dt, \quad (7)$$

where $q^A(x_t)$ is the marginal distribution of Q^A at time t .

This allows one to estimate the KL divergence between two diffusions with the same volatility coefficient and the same initial distributions, knowing only their *drifts* and marginal samples $x_t \sim q^A(x_t)$. This fact is widely used in Bridge Matching (Shi et al., 2023; Peluchetti, 2023), Diffusion (Franzese et al., 2024) and Schrödinger Bridge Models (Vargas et al., 2021; Gushchin et al., 2023).

3. Related Work

Mutual information estimators. Mutual information estimators fall into two main categories: *non-parametric* and *parametric*. Parametric estimators are also subdivided into *discriminative* and *generative* (Song & Ermon, 2020; Federici et al., 2023). In addition to this natural classification, we distinguish *diffusion-based* approaches to better contextualize our method in relation to the previous works.

Non-parametric estimators. Classical approaches to the mutual information estimation rely on non-parametric density estimators, such as kernel density estimator (Weglarczyk, 2018; Goldfeld et al., 2019) and k -nearest neighbors estimator (Kozachenko & Leonenko, 1987; Kraskov et al., 2004; Berrett et al., 2019). The resulting density estimate is plugged into (2) to acquire the MI estimate through MC-integration, leave-one-out method or other techniques. The simplicity of such methods make them appealing for low-dimensional cases, but extensive high-dimensional evaluation suggests that these approaches are inapplicable to complex data (Goldfeld et al. 2019, § 5.3; Czyż et al. 2023, § 6.2; Butakov et al. 2024a, Table 1).

Non-diffusion-based generative estimators. More advanced techniques involve parametric density models, such as normalizing flows and variational autoencoders, to measure MI through density estimation. This naïve generative approach was described by (Song & Ermon, 2020; McAllester & Stratos, 2020) and further investigated in the works of (Ao & Li, 2022; Duong & Nguyen, 2023a). However, despite better modelling capabilities, the results in (Song & Ermon, 2020, Figures 1,2) indicate that direct PDF estimation can introduce a substantial bias to the MI estimate. Therefore, it was proposed to avoid PDF estimation altogether and focus on measuring the density ratio in (2). This is done in the works of (Duong & Nguyen, 2023a; Butakov et al., 2024a) by leveraging the invariance property of

mutual information. Such methods show better performance on synthetic benchmarks, but may introduce an inductive bias due to the simplified closed-form expression being used to estimate the density ratio in question.

Discriminative estimators. Finally, another approach to MI estimation involves training a classifier to discriminate between the samples from Π_{X_0, X_1} and $\Pi_{X_0} \otimes \Pi_{X_1}$: MINE (Belghazi et al., 2018), InfoNCE (van den Oord et al., 2019) and similar methods (Song & Ermon, 2020). This technique leverages variational bounds on the Kullback-Leibler divergence and provides a relatively cheap and reliable parametric estimator for a wide range of cases, including high-dimensional and complex data. However, such estimators have severe demerits from a theoretical perspective, such as high variance in MINE and large batch size requirements in InfoNCE (Song & Ermon, 2020). Additionally, recent benchmarking results suggest that discriminative approaches can underperform compared to the generative methods when MI is high and the probability distribution is complex (Franzese et al., 2024; Butakov et al., 2024a).

Neural Diffusion Estimator for MI (MINDE). One of the most recent generative methods for MI Estimation is diffusion-based (Song et al., 2021) MINDE (Franzese et al., 2024). To estimate $\text{KL}(\pi^A \parallel \pi^B)$ the authors learn two standard backward diffusion models to generate data from distributions π^A and π^B , e.g., for π^A :

$$\begin{cases} Q^A : \underbrace{dx_t = [-f(x_t, t) + g(t)^2 s^A(x_t, t)]dt + g(t)d\hat{W}_t}_{\text{backward diffusion}}, \\ x_T \sim q_T^A(x_T), \end{cases} \quad (8)$$

where f and g are the drift and volatility coefficients, respectively, of the forward diffusion (Song et al., 2021), $d\hat{W}_t$ is the Wiener process when time flows backwards, and q_t^A is the distribution of the noised data at time t (Franzese et al., 2024, §2, 3). The similar expressions hold for π^B and Q^B . Then, the authors formulate a KL divergence estimator through the difference of diffusion *score functions*:

$$\begin{aligned} \text{KL}(\pi^A \parallel \pi^B) &= \text{KL}(Q^A \parallel Q^B) = \\ &\int_0^T \mathbb{E}_{q_t^A(x_t|x_0)} \left[\frac{g(t)^2}{2} \|s^A(x_t, t) - s^B(x_t, t)\|^2 \right] dt + \\ &\quad \text{KL}(q_T^A \parallel q_T^B). \end{aligned} \quad (9)$$

Here, $\text{KL}(q_T^A \parallel q_T^B)$ is the **bias** term, which vanishes only when diffusion has infinitely many steps, i.e., $T \rightarrow \infty$. When the diffusion score functions s^A and s^B (8) are properly learned, one can draw samples from the forward diffusion $q_t^A(x_t|x_0)$ and compute the estimate of KL divergence (9). In this way, the authors transform the problem of training the KL divergence estimator into the problem of learning the backward diffusions (8) that generate *data from noise*.

To estimate mutual information, the authors propose a total of four equivalent methods, all based on the estimation of up to three KL divergences (9) or their expectations.

4. InfoBridge Mutual Information estimator

In §4.1, we propose our novel MI estimator which is based on difference of diffusion drifts of conditional reciprocal processes. Suggest some straightforward generalizations in §4.2. Explain the practical learning procedure in §4.3.

4.1. Computing MI through Reciprocal Processes

Consider the problem of MI estimation for random variables X_0 and X_1 with joint distribution $\pi(x_0, x_1)$. To tackle this problem, we employ reciprocal processes:

$$Q_\pi \stackrel{\text{def}}{=} \int W_{|x_0, x_1}^\epsilon d\pi(x_0, x_1), \quad (10)$$

$$Q_\pi^{\text{ind}} \stackrel{\text{def}}{=} \int W_{|x_0, x_1}^\epsilon d\pi(x_0) d\pi(x_1). \quad (11)$$

We show that the KL between the distributions $\pi(x_0, x_1)$ and $\pi(x_0)\pi(x_1)$ (1) is equal to the KL between the reciprocal processes Q_π and Q_π^{ind} , and decompose the latter into the difference of drifts.

Theorem 4.1 (Mutual Information decomposition). *Consider random variables X_0, X_1 , with joint distribution $\pi(x_0, x_1)$. Consider reciprocal processes $Q_\pi, Q_\pi^{\text{ind}}$ induced by distributions $\pi(x_0, x_1)$ and $\pi(x_0)\pi(x_1)$, respectively, as in (10) (11). Then the mutual information between the random variables X_0 and X_1 can be expressed as:*

$$\begin{aligned} I(X_0; X_1) &= \\ &= \frac{1}{2\epsilon} \int_0^1 \mathbb{E}_{q_\pi(x_t, x_0)} \|v_{\text{joint}}(x_t, t, x_0) - v_{\text{ind}}(x_t, t, x_0)\|^2 dt, \end{aligned} \quad (12)$$

where

$$v_{\text{joint}}(x_t, t, x_0) = \mathbb{E}_{x_1 \sim q_\pi(x_1|x_t, x_0)} \left[\frac{x_1 - x_t}{1 - t} \right], \quad (13)$$

$$v_{\text{ind}}(x_t, t, x_0) = \mathbb{E}_{x_1 \sim q_\pi^{\text{ind}}(x_1|x_t, x_0)} \left[\frac{x_1 - x_t}{1 - t} \right]. \quad (14)$$

v_{joint} and v_{ind} are the drifts of the SDE representations (4) of the reciprocal processes Q_π and Q_π^{ind} .

Proof. Using the disintegration theorem (Léonard, 2014, §1) at time $t = 0$, we get:

$$\begin{aligned} \text{KL}(Q_\pi \parallel Q_\pi^{\text{ind}}) &= \text{KL}(\pi(x_0) \parallel \pi(x_0)) + \\ &+ \mathbb{E}_{\pi(x_0)} [\text{KL}(Q_{\pi|x_0} \parallel Q_{\pi^{\text{ind}}|x_0})]. \end{aligned}$$

Note that since $Q_\pi, Q_\pi^{\text{ind}}$ share the same marginals at time $t = 0$, first KL term vanishes. Similarly, by using the disintegration theorem again for both times $t = 0, 1$, we get:

Algorithm 1: InfoBridge. MI estimator.

Input : Distribution $\pi(x_0, x_1)$ accessible by samples,
 neural network parametrization v_θ of drift
 functions approximating optimal drifts v_{joint}
 and v_{ind} , number of samples N

Output : Mutual information estimation $\widehat{\text{MI}}$

Sample batch of pairs $\{x_0^n, x_1^n\}_{n=0}^N \sim \pi(x_0, x_1)$;

Sample batch $\{t^n\}_{n=0}^N \sim U[0, 1]$;

Sample batch $\{x_t^n\}_{n=0}^N \sim W_{|x_0, x_1}^\epsilon$;

$\widehat{\text{MI}} \leftarrow$

$$\frac{1}{2\epsilon N} \sum_{n=0}^N \|v_\theta(x_t^n, t^n, x_0^n, 1) - v_\theta(x_t^n, t^n, x_0^n, 0)\|^2$$

$$\begin{aligned} \text{KL}(Q_\pi \| Q_\pi^{\text{ind}}) &= \text{KL}(\pi(x_0, x_1) \| \pi(x_0)\pi(x_1)) + \\ &+ \mathbb{E}_{\pi(x_0, x_1)} \left[\text{KL}\left(Q_{\pi|x_0, x_1} \| Q_{\pi|x_0, x_1}^{\text{ind}}\right) \right]. \end{aligned}$$

Recap that Q_π and Q_π^{ind} are both mixtures of Brownian Bridges. Therefore, $Q_{\pi|x_0, x_1} = Q_{\pi|x_0, x_1}^{\text{ind}} = W_{|x_0, x_1}^\epsilon$ and

$\text{KL}\left(Q_{\pi|x_0, x_1} \| Q_{\pi|x_0, x_1}^{\text{ind}}\right) = 0$. Then the following holds:

$$\begin{aligned} \text{KL}(Q_\pi \| Q_\pi^{\text{ind}}) &= \text{KL}(\pi(x_0, x_1) \| \pi(x_0)\pi(x_1)) = \\ &= \mathbb{E}_{\pi(x_0)} \left[\text{KL}\left(Q_{\pi|x_0} \| Q_{\pi|x_0}^{\text{ind}}\right) \right]. \end{aligned}$$

Moreover, processes $Q_{\pi|x_0}$ and $Q_{\pi|x_0}^{\text{ind}}$ are diffusion processes (§2). Then, by recalling (7), we get:

$$\begin{aligned} \text{KL}(\pi(x_0, x_1) \| \pi(x_0)\pi(x_1)) &= \\ &= \mathbb{E}_{\pi(x_0)} \left[\text{KL}\left(Q_{\pi|x_0} \| Q_{\pi|x_0}^{\text{ind}}\right) \right] = \end{aligned} \quad (15)$$

$$\frac{1}{2\epsilon} \int_0^1 \mathbb{E}_{q_\pi(x_t, x_0)} \left[\|v_{\text{joint}}(x_t, t, x_0) - v_{\text{ind}}(x_t, t, x_0)\|_2^2 \right] dt,$$

where drifts v_{joint} and v_{ind} are defined as in (13) and (14) respectively. \square

Once the drifts v_{joint} and v_{ind} are known, our Theorem 4.1 provides a straightforward way to estimate the mutual information between the random variables X_0 and X_1 by evaluating the difference between the drifts $v_{\text{joint}}(x_t, t, x_0)$ (13) and $v_{\text{ind}}(x_t, t, x_0)$ (14) at points x_t sampled from the distribution of the reciprocal process Q_π at times 0, t . Similar formulas can be derived for the estimation of pointwise mutual information, see Appendix A.3.

4.2. Possible generalizations

Our method admits several straightforward extensions. For completeness, we present a method for unbiased estimation of the general KL divergence in Appendix A.1. According to the Theorem A.1 the KL divergence between any two distributions can be decomposed into the difference of diffusion

Algorithm 2: InfoBridge. Training the model.

Input : Distribution $\pi(x_0, x_1)$ accessible by samples,
 initial neural network parametrization v_θ of
 drift functions

Output : Learned neural network v_θ approximating
 optimal drifts v_{joint} and v_{ind}

repeat

Sample batch of pairs $\{x_0^n, x_1^n\}_{n=0}^N \sim \pi(x_0, x_1)$;

Sample random permutation

$\{\hat{x}_1^n\}_{n=0}^N = \text{Permute}(\{x_1^n\}_{n=0}^N)$;

Sample batch $\{t^n\}_{n=0}^N \sim U[0, 1]$;

Sample batch $\{x_t^n\}_{n=0}^N \sim W_{|x_0, x_1}^\epsilon$;

Sample batch $\{\hat{x}_t^n\}_{n=0}^N \sim W_{|x_0, \hat{x}_1}^\epsilon$;

$\mathcal{L}_\theta^1 = \frac{1}{N} \sum_{n=1}^N \|v_\theta(x_t^n, t^n, x_0^n, 1) - \frac{x_1^n - x_t^n}{1 - t^n}\|_2^2$;

$\mathcal{L}_\theta^2 = \frac{1}{N} \sum_{n=1}^N \|v_\theta(\hat{x}_t^n, t^n, x_0^n, 0) - \frac{\hat{x}_1^n - \hat{x}_t^n}{1 - t^n}\|_2^2$;

Update θ using $\frac{\partial \mathcal{L}_\theta^1}{\partial \theta} + \frac{\partial \mathcal{L}_\theta^2}{\partial \theta}$;

until converged;

drifts in similar way to (12). In addition, this results allows for the estimation of differential entropy of any probability distribution, see Appendix A.2.

In addition, our method can be extended to estimate mutual information involving more than two random variables, known as interaction information (Appendix A.4). Practical procedures for these generalizations can be derived in a similar way to §4.3.

4.3. InfoBridge. Practical optimization procedure

The drifts v_{joint} and v_{ind} of reciprocal processes Q_π and Q_π^{ind} can be recovered by the conditional Bridge Matching procedure, see §2. We have to solve optimization problem (6) by parametrizing v_{joint} and v_{ind} with neural networks $v_{\text{joint}, \phi}$ and $v_{\text{ind}, \psi}$, respectively, and applying Stochastic Gradient Descent on Monte Carlo approximation of (6). The sampling from the distribution $q_\pi(x_t, x_0)$ of reciprocal process Q_π at times 0, t is easy because:

$$\begin{aligned} q_\pi(x_t, x_0) &= \mathbb{E}_{q_\pi(x_1)} [q_\pi(x_t, x_0 | x_1)] = \\ &= \mathbb{E}_{q_\pi(x_1)} [q_\pi(x_t | x_1, x_0) \pi(x_0 | x_1)]. \end{aligned}$$

Therefore, to sample from $q_\pi(x_t, x_0)$ it suffices to sample $x_0, x_1 \sim \pi(x_0, x_1)$ and sample from $q_\pi(x_t | x_1, x_0)$ which is again just a Brownian Bridge.

Generative byproduct. Note that the learned drifts $v_{\text{joint}, \phi}$ and $v_{\text{ind}, \psi}$ define the distributions $\pi_\phi(x_1 | x_0) \approx \pi(x_1 | x_0)$ and $\pi_\psi(x_1 | x_0) \approx \pi(x_1)$ as solutions to the corresponding SDEs (4). One can sample from these distributions by solving the related SDE (4) numerically, e.g., using the Euler-Maryama solver (Kloeden, 1992). Despite this being unnecessary for our MI estimation, it can be considered as an additional feature.

Mutual Information estimation via Bridge Matching

Method	0.2	0.4	0.3	0.4	0.4	0.4	0.4	1.0	1.0	1.0	1.0	0.3	1.0	1.3	1.0	0.4	1.0	0.6	1.6	0.4	1.0	1.0	1.0	1.0	1.0	1.0	1.0	1.0	1.0	0.2	0.4	0.2	0.3	0.2	0.4	0.3	0.4	1.7	0.3	0.4
GT	0.2	0.4	0.3	0.4	0.4	0.4	0.4	1.0	1.0	1.0	1.0	0.3	1.0	1.3	1.0	0.4	1.0	0.6	1.6	0.4	1.0	1.0	1.0	1.0	1.0	1.0	1.0	1.0	1.0	0.2	0.4	0.2	0.3	0.2	0.4	0.3	0.4	1.7	0.3	0.4
InfoBridge	0.3	0.5	0.3	0.4	0.4	0.4	0.9	1.0	1.0	1.0	0.3	1.0	1.3	1.0	0.4	1.0	0.6	1.7	0.4	1.0	1.0	1.0	1.0	0.9	0.9	1.0	1.0	0.0	0.0	0.2	0.3	0.2	0.5	0.3	0.5	1.3	0.4	0.4		
MINDE-J ($\sigma = 1$)	0.2	0.4	0.3	0.4	0.4	0.4	1.1	1.0	1.0	1.0	0.3	0.9	1.2	1.0	0.4	1.0	0.6	1.7	0.4	1.0	1.0	1.0	0.9	0.9	0.9	1.0	0.9	1.0	0.2	0.4	0.2	0.3	0.2	0.5	0.3	0.5	1.6	0.3	0.4	
MINDE-J	0.2	0.4	0.3	0.4	0.4	0.4	1.2	1.0	1.0	1.0	0.3	1.0	1.3	1.0	0.4	1.0	0.6	1.7	0.4	1.1	1.0	1.0	0.9	0.9	1.1	1.0	1.0	0.1	0.2	0.2	0.3	0.2	0.5	0.3	0.4	1.7	0.3	0.4		
MINDE-c ($\sigma = 1$)	0.2	0.4	0.3	0.4	0.4	0.4	1.0	1.0	1.0	1.0	0.3	1.0	1.3	1.0	0.4	1.0	0.6	1.6	0.4	0.9	1.0	1.0	0.9	0.9	0.9	1.0	0.9	0.1	0.3	0.2	0.3	0.2	0.4	0.3	0.3	1.7	0.3	0.4		
MINDE-c	0.2	0.4	0.3	0.4	0.4	0.4	1.0	1.0	1.0	1.0	0.3	1.0	1.3	1.0	0.4	1.0	0.6	1.6	0.4	1.0	1.0	1.0	0.9	0.9	1.0	1.0	1.0	0.1	0.3	0.2	0.3	0.2	0.4	0.3	0.4	1.7	0.3	0.4		
MINE	0.2	0.4	0.2	0.4	0.4	0.4	1.0	1.0	1.0	1.0	0.3	1.0	1.3	1.0	0.4	1.0	0.6	1.6	0.4	0.9	0.9	0.9	0.8	0.7	0.6	0.9	0.9	0.9	0.0	0.0	0.1	0.1	0.1	0.2	0.2	0.4	1.7	0.3	0.4	
InfoNCE	0.2	0.4	0.3	0.4	0.4	0.4	1.0	1.0	1.0	1.0	0.3	1.0	1.3	1.0	0.4	1.0	0.6	1.6	0.4	0.9	1.0	1.0	0.8	0.8	0.8	0.9	1.0	1.0	0.2	0.3	0.2	0.3	0.2	0.4	0.3	0.4	1.7	0.3	0.4	
D-V	0.2	0.4	0.3	0.4	0.4	0.4	1.0	1.0	1.0	1.0	0.3	1.0	1.3	1.0	0.4	1.0	0.6	1.6	0.4	0.9	1.0	1.0	0.8	0.8	0.8	0.9	1.0	1.0	0.0	0.0	0.1	0.1	0.2	0.2	0.2	0.4	1.7	0.3	0.4	
NWJ	0.2	0.4	0.3	0.4	0.4	0.4	1.0	1.0	1.0	1.0	0.3	1.0	1.3	1.0	0.4	1.0	0.6	1.6	0.4	0.9	1.0	1.0	0.8	0.8	0.8	0.9	1.0	1.0	0.0	0.0	0.0	-0.6	0.1	0.1	0.2	0.4	1.7	0.3	0.4	
DoE(Gaussian)	0.2	0.5	0.3	0.6	0.4	0.4	0.4	0.7	1.0	1.0	0.4	0.7	0.7	0.8	1.0	0.6	0.9	1.3	0.4	0.7	1.0	1.0	0.5	0.6	0.6	0.6	0.7	0.8	6.7	7.9	1.8	2.5	0.6	4.2	1.2	1.6	0.1	0.4		
DoE(Logistic)	0.1	0.4	0.2	0.4	0.4	0.4	0.6	0.9	0.9	1.0	0.3	0.7	0.7	0.8	1.0	0.6	0.9	1.3	0.4	0.8	1.1	1.0	0.5	0.6	0.6	0.7	0.8	0.8	0.5	0.8	0.3	1.5	0.6	1.6	0.1	0.4				
KSG	0.2	0.4	0.2	0.2	0.4	0.4	0.4	0.2	0.9	0.7	1.0	0.3	0.2	1.1	1.0	0.4	0.7	0.6	1.3	0.4	0.2	0.9	0.7	0.2	0.7	0.6	0.2	0.9	0.7	0.2	0.2	0.1	0.1	0.1	0.2	0.2	0.4	1.7	0.3	0.4

Wiegly @ Bivariate Mn 1×1
 Uniform 1×1 (additive noise=0.75)
 Uniform 1×1 (additive noise=0.1)
 Swiss roll 2×1
 Sr 5×5 (dot=3)
 Sr 5×5 (dot=2)
 Sr 3×3 (dot=3)
 Sr 3×3 (dot=2)
 Sr 2×2 (dot=2)
 Sr 2×2 (dot=1)
 Sr 1×1 (dot=1)
 Sp @ Mn CDF @ Mn 5×5 (2-pair)
 Sp @ Mn CDF @ Mn 3×3 (2-pair)
 Sp @ Mn CDF @ Mn 25×25 (2-pair)
 Sp @ Mn 5×5 (2-pair)
 Sp @ Mn 3×3 (2-pair)
 Sp @ Mn 25×25 (2-pair)
 Mn CDF @ Mn 5×5 (2-pair)
 Mn CDF @ Mn 3×3 (2-pair)
 Mn CDF @ Mn 25×25 (2-pair)
 Mn CDF @ Bivariate Mn 1×1
 Mn 50×50 (dense)
 Mn 5×5 (dense)
 Mn 5×5 (2-pair)
 Mn 3×3 (dense)
 Mn 3×3 (2-pair)
 Mn 25×25 (dense)
 Mn 25×25 (2-pair)
 Mn 2×2 (dense)
 Mn 2×2 (2-pair)
 Hc @ Mn 5×5 (2-pair)
 Hc @ Mn 3×3 (2-pair)
 Hc @ Mn 25×25 (2-pair)
 Hc @ Bivariate Mn 1×1
 Bivariate Mn 1×1
 Bimodal 1×1
 Asinh @ Sr 5×5 (dot=2)
 Asinh @ Sr 3×3 (dot=2)
 Asinh @ Sr 2×2 (dot=1)
 Asinh @ Sr 1×1 (dot=1)

Table 1: Mean MI estimates over 10 seeds using 10k test samples against ground truth (GT), adopted from (Franzese et al., 2024). Color indicates relative negative (red) and positive bias (blue). Size of train dataset for every neural method is 100k. All the methods for comparison with *InfoBridge* were taken from (Czyż et al., 2023; Franzese et al., 2024). List of abbreviations (*Mn*: Multinormal, *Sr*: Student-t, *Nm*: Normal, *Hc*: Half-cube, *Sp*: Spiral)

Vector field parametrization. In practice, we replace two separate neural networks that approximate the drifts $v_{\text{joint}}(x_t, t, x_0)$ and $v_{\text{ind}}(x_t, t, x_0)$ with a single neural network that incorporates an additional binary input. Specifically, we introduce a binary input $s \in \{0, 1\}$ to unify the drift approximations in the following way: $v_{\theta}(\cdot, 1) \approx v_{\text{joint}}(\cdot)$ and $v_{\theta}(\cdot, 0) \approx v_{\text{ind}}(\cdot)$. The introduction of an additional input is widely used for the conditioning of diffusion (Ho & Salimans, 2021) and bridge matching (Bortoli et al., 2024) models. We have empirically found that it provides a much more accurate estimation of mutual information. We attribute its performance to the fact that for MI estimation we need to compute the difference between diffusion drifts (12). Neural networks are usually not ideal and have some approximation error, then the difference between two almost identical neural networks with similar approximation errors is more accurate than the difference between two neural networks with distinct approximation errors.

We call our practical MI estimation algorithm *InfoBridge*, provide the drifts training procedure in Algorithm 2 and describe the MI estimation procedure in Algorithm 1.

5. Experiments

We test our method on a diverse set of benchmarks with already known ground truth value of MI. To cover low-dimensional cases, long-tailed distributions and some basic

cases of data lying on a manifold, we employ the tests by Czyż et al. (2023). Benchmarks from (Butakov et al., 2024b;a) are used to assess the method on manifolds represented as images.

Low-dimensional benchmark. The tests from (Czyż et al., 2023) focus on low-dimensional distributions with tractable mutual information. Various mappings are also applied to make the distributions light- or heavy-tailed, or to non-linearly embed the data into an ambient space of higher dimensionality.

InfoBridge is tested with $\epsilon = 1$ and a multi-layer dense neural network is used to approximate the drifts. Our computational complexity is comparable to MINDE (Franzese et al., 2024). For more details, please, refer to Appendix B. In each test, we perform 10 independent runs with 100k train set samples and 10k test set samples. The mean MI estimation results are reported in the top row of Tables 1 and 4.

Overall, the performance of our estimator is similar to that of MINDE §3, with the Cauchy distribution (i.e., Student-t distribution with degrees of freedom equal to 1) being the only notable exception. The Cauchy distribution lacks the first moment, which poses theoretical limitations for Bridge Matching (Shi et al., 2023, Appendix C). Additionally, its heavy tails make the estimation of mutual information more

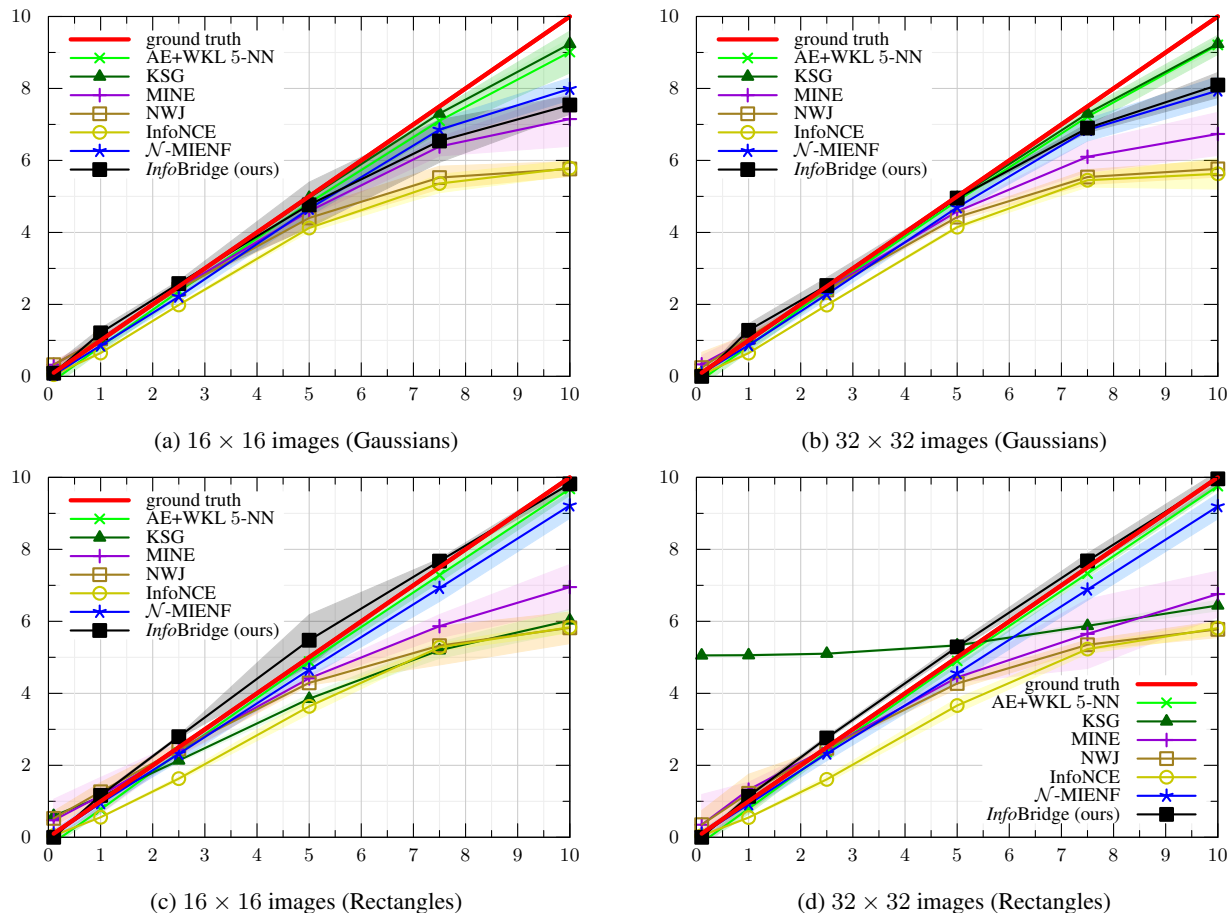


Figure 1: Comparison of the selected estimators. Along x axes is $I(X_0; X_1)$, along y axes is MI estimate $\hat{I}(X_0; X_1)$. We plot 99% asymptotic CIs acquired from different seed runs. Number of seeds for *InfoBridge* and \mathcal{N} -MIENF is 3 and 5 for all the other methods. 100k samples were used for neural methods training and 10k for validation.

challenging. Figures 7 and 8 in (Franzese et al., 2024) indicate that MINDE also faces difficulties in providing a reliable estimate in this specific scenario, and it is likely that it should not perform effectively in theory with Cauchy distribution either. However, using the tail-shortening asinh transform allows our method to estimate MI almost accurately, see Tables 1 and 4.

Image data benchmark. In (Butakov et al., 2024b), it was proposed to map low-dimensional distributions with tractable MI into manifolds admitting image-like structure, thus producing synthetic images (in particular, images of 2D Gaussians and Rectangles, see Figures 2a and 2b). By using smooth injective mappings, one ensures that MI is not alternated by the transform (Butakov et al., 2024a, Theorem 2.1). In the original works, it is argued that such benchmarks are closer to real data, and therefore give more insights into the problems related to the MI estimation in realistic setups.

Each neural algorithm is trained with 100k train set samples and validated using 10k samples. *InfoBridge* is tested with

$\epsilon = 1$ and we use a neural network with U-net architecture (Ronneberger et al., 2015) to approximate the drift. For averaging, we run algorithm with 3 different seeds. Other experimental details are reported in Appendix B.2.

We present our results for 16×16 and 32×32 resolution images with both Gaussian and rectangle structure in Figure 1, while the samples from the learned conditional bridge matching models can be viewed in Figures 2c to 2f. Our estimator looks very competitive, being as good as or even better than two previous best-performing methods: Mutual Information Estimation via Normalizing Flows (MIENF) (Butakov et al., 2024a) and 5-nearest neighbors weighted Kozachenko-Leonenko estimator (Kozachenko & Leonenko, 1987; Berrett et al., 2019) fed with autoencoder-generated embeddings (AE+WKL 5-NN) (Butakov et al., 2024b). We consider this to be a satisfactory outcome, since MIENF and AE+WKL utilize certain prior information about the test (specifically, the vector Gaussian copula structure in \mathcal{N} -MIENF (Butakov et al., 2024a, Section

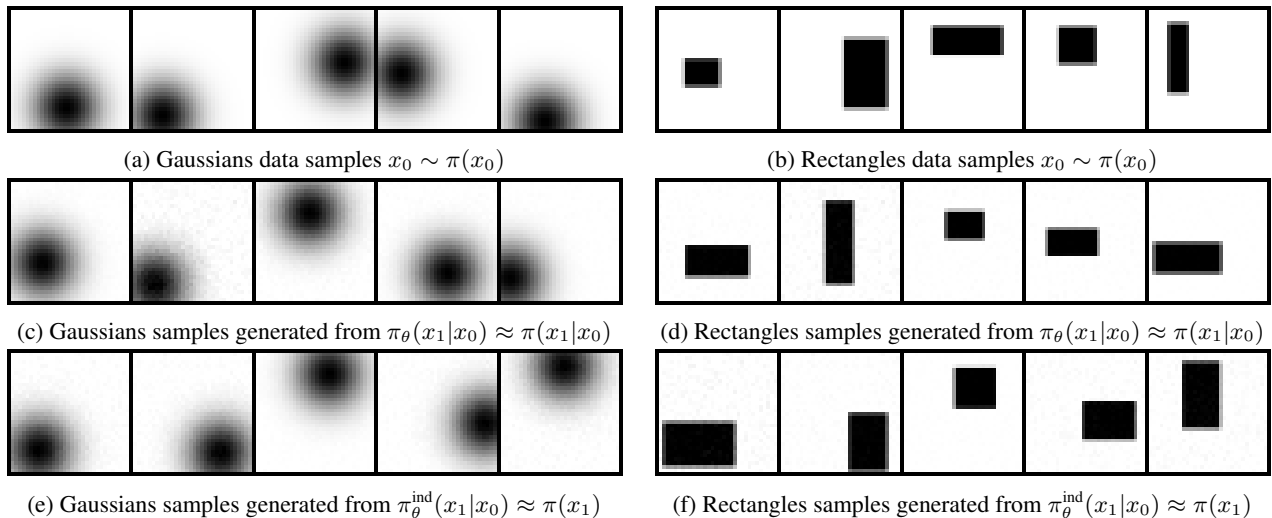


Figure 2: Examples of synthetic images from the (Butakov et al., 2024a) benchmark can be seen at Figures 2a and 2b. Note that images are high-dimensional, but admit latent structure, which is similar to real datasets. Samples generated from the learned distributions $\pi_\theta(x_1|x_0) \approx \pi(x_1|x_0)$ and $\pi_\theta^{\text{ind}}(x_1|x_0) \approx \pi(x_1)$ defined as solutions to SDEs (4) with approximated drifts $v_\theta(\cdot, 0)$ and $v_\theta(\cdot, 1)$, respectively, can be seen at Figures 2c to 2f. All the images have 32×32 resolution.

B, paragraph 1),¹ or the low intrinsic dimensionality in AE+WKL²), while our estimator remains *free of any inductive bias*. Moreover, as a result of the tests conducted, we claim that our estimator is *the best among all bias-free estimators* featured.

6. Discussion

Potential Impact. Our contributions include the development of novel unbiased estimator for the MI grounded in diffusion bridge matching theory. The proposed algorithm, *InfoBridge*, demonstrates superior performance compared to commonly used MI estimators without inductive bias on challenging image-based benchmarks. Also, our approach can be used to estimate the KL divergence, and differential entropy, see Appendices A.1 and A.2.

We believe that this work paves the way for new directions in the estimation of MI *in high dimensions*. This has potential real-world applications such as text-to-image alignment (Wang et al., 2024), self-supervised learning (Bachman et al., 2019), deep neural network analysis (Butakov et al., 2024b), and other use cases in high-dimensional settings.

Moreover, this approach offers *significant opportunities for extension* by exploring alternative types of bridges within

¹ \mathcal{N} -MIENF requires $\Pi_{X,Y}$ being gaussianizable via some Cartesian product mapping $f_X \times f_Y$; the analysis provided in (Czyż et al., 2025) suggests that this is a strong implication, which is extremely unlikely to be satisfied in non-synthetic cases.

²For this estimator, we use the experimental setup from (Butakov et al., 2024b), which skews the comparison against us since the autoencoder bottlenecks match the true intrinsic dimensionality of the data. We show the degenerated performance of WKL in a slightly alternated setup in Appendix B.3.

reciprocal processes. For instance, variance-preserving stochastic differential equations (SDEs) could be used instead of the Brownian motion (Zhou et al., 2024). In addition, experimentation with different volatility coefficients ϵ (Liu et al., 2023) or advanced diffusion bridge techniques, such as time reweighting (Kim et al., 2025), could further improve the methodology. Finally, for long-tailed data distributions, it may be possible to integrate long-tailed diffusion techniques (Yoon et al., 2023), extending the applicability of our approach to even more complex settings.

Limitations. Our approach is fundamentally based on the diffusion bridge matching framework. While this class of models and its theoretical foundations have demonstrated strong potential in high-dimensional generative modeling (Shi et al., 2023; Liu et al., 2023; Song et al., 2021), they also have certain limitations that, while often negligible in the context of generative modeling, can be more pronounced in other applications.

One such limitation, evident in our work, is the challenge of accurately approximating heavy-tailed distributions. As can be seen in Table 1, one-degree-of-freedom Student-t distribution, i.e., $St(\text{dof}=1)$, also known as Cauchy distribution, has no first moment, and our method is not applicable to such distributions in theory (Shi et al., 2023, Appendix C). However, worth noting that such limitations are quite common for generative modeling and quite probably should be applicable to denoising score matching and diffusion models as well (Franzese et al., 2024; Song et al., 2021). Another limitation of diffusion (and diffusion bridge matching models as a consequence) is that it requires a lot of data samples at training stage. This could hinder the applicability of our method with low number of data samples.

Broader impact. This paper presents work whose goal is to advance the field of Machine Learning. There are many potential societal consequences of our work, none of which we feel must be specifically highlighted here.

References

- Amjad, R. A., Liu, K., and Geiger, B. C. Understanding neural networks and individual neuron importance via information-ordered cumulative ablation. *IEEE Transactions on Neural Networks and Learning Systems*, 33(12): 7842–7852, 2022. doi: 10.1109/TNNLS.2021.3088685.
- Ao, Z. and Li, J. Entropy estimation via normalizing flow. *Proceedings of the AAAI Conference on Artificial Intelligence*, 36(9):9990–9998, Jun. 2022. doi: 10.1609/aaai.v36i9.21237. URL <https://ojs.aaai.org/index.php/AAAI/article/view/21237>.
- Ardizzone, L., Mackowiak, R., Rother, C., and Köthe, U. Training normalizing flows with the information bottleneck for competitive generative classification. In Larochelle, H., Ranzato, M., Hadsell, R., Balcan, M., and Lin, H. (eds.), *Advances in Neural Information Processing Systems*, volume 33, pp. 7828–7840. Curran Associates, Inc., 2020. URL https://proceedings.neurips.cc/paper_files/paper/2020/file/593906af0d138e69f49d251d3e7cbcd0-Paper.pdf.
- Bachman, P., Hjelm, R. D., and Buchwalter, W. Learning representations by maximizing mutual information across views. In Wallach, H., Larochelle, H., Beygelzimer, A., d'Alché-Buc, F., Fox, E., and Garnett, R. (eds.), *Advances in Neural Information Processing Systems*, volume 32. Curran Associates, Inc., 2019. URL https://proceedings.neurips.cc/paper_files/paper/2019/file/ddf354219aac374f1d40b7e760ee5bb7-Paper.pdf.
- Baram, N., Tennenholtz, G., and Mannor, S. Action redundancy in reinforcement learning. In de Campos, C. and Maathuis, M. H. (eds.), *Proceedings of the Thirty-Seventh Conference on Uncertainty in Artificial Intelligence*, volume 161 of *Proceedings of Machine Learning Research*, pp. 376–385. PMLR, 27–30 Jul 2021. URL <https://proceedings.mlr.press/v161/baram21a.html>.
- Belghazi, M. I., Baratin, A., Rajeshwar, S., Ozair, S., Bengio, Y., Courville, A., and Hjelm, D. Mutual information neural estimation. In Dy, J. and Krause, A. (eds.), *Proceedings of the 35th International Conference on Machine Learning*, volume 80 of *Proceedings of Machine Learning Research*, pp. 531–540. PMLR, 07 2018. URL <https://proceedings.mlr.press/v80/belghazi18a.html>.
- Bell, A. J. and Sejnowski, T. J. An information-maximization approach to blind separation and blind deconvolution. *Neural Comput.*, 7(6):1129–1159, November 1995.
- Berrett, T. and Samworth, R. Nonparametric independence testing via mutual information. *Biometrika*, 106, 11 2017. doi: 10.1093/biomet/asz024.
- Berrett, T. B., Samworth, R. J., and Yuan, M. Efficient multivariate entropy estimation via k -nearest neighbour distances. *Ann. Statist.*, 47(1):288–318, 02 2019. doi: 10.1214/18-AOS1688. URL <https://doi.org/10.1214/18-AOS1688>.
- Bortoli, V. D., Korshunova, I., Mnih, A., and Doucet, A. Schrodinger bridge flow for unpaired data translation. In *The Thirty-eighth Annual Conference on Neural Information Processing Systems*, 2024. URL <https://openreview.net/forum?id=1F32iCJFfa>.
- Bounoua, M., Franzese, G., and Michiardi, P. \mathbb{S}^1 : Score-based o-INFORMATION estimation. In Salakhutdinov, R., Kolter, Z., Heller, K., Weller, A., Oliver, N., Scarlett, J., and Berkenkamp, F. (eds.), *Proceedings of the 41st International Conference on Machine Learning*, volume 235 of *Proceedings of Machine Learning Research*, pp. 4444–4471. PMLR, 21–27 Jul 2024a. URL <https://proceedings.mlr.press/v235/bounoua24a.html>.
- Bounoua, M., Franzese, G., and Michiardi, P. \mathbb{S}^1 : Score-based o-information estimation. In *ICML 2024, 41st International Conference on Machine Learning*, 2024b.
- Bunne, C., Hsieh, Y.-P., Cuturi, M., and Krause, A. The schrödinger bridge between gaussian measures has a closed form. In *International Conference on Artificial Intelligence and Statistics*, pp. 5802–5833. PMLR, 2023.
- Butakov, I., Tolmachev, A., Malanchuk, S., Neopryatnaya, A., and Frolov, A. Mutual information estimation via normalizing flows. In *The Thirty-eighth Annual Conference on Neural Information Processing Systems*, 2024a. URL <https://openreview.net/forum?id=JiQXsLvDls>.
- Butakov, I., Tolmachev, A., Malanchuk, S., Neopryatnaya, A., Frolov, A., and Andreev, K. Information bottleneck analysis of deep neural networks via lossy compression. In *The Twelfth International Conference on Learning Representations*, 2024b. URL <https://openreview.net/forum?id=huGECz8dPp>.

- Chen, X., Duan, Y., Houthoofd, R., Schulman, J., Sutskever, I., and Abbeel, P. Infogan: Interpretable representation learning by information maximizing generative adversarial nets. In Lee, D. D., Sugiyama, M., von Luxburg, U., Guyon, I., and Garnett, R. (eds.), *Advances in Neural Information Processing Systems 29: Annual Conference on Neural Information Processing Systems 2016, December 5-10, 2016, Barcelona, Spain*, pp. 2172–2180, 2016. URL <https://proceedings.neurips.cc/paper/2016/hash/7c9d0b1f96aebd7b5eca8c3edaa19ebb-Abstract.html>.
- Chen, Z., He, G., Zheng, K., Tan, X., and Zhu, J. Schrodinger bridges beat diffusion models on text-to-speech synthesis. *arXiv preprint arXiv:2312.03491*, 2023.
- Cover, T. M. and Thomas, J. A. *Elements of Information Theory (Wiley Series in Telecommunications and Signal Processing)*. Wiley-Interscience, USA, 2006.
- Cunningham, E., Cobb, A. D., and Jha, S. Principal component flows. In Chaudhuri, K., Jegelka, S., Song, L., Szepesvari, C., Niu, G., and Sabato, S. (eds.), *Proceedings of the 39th International Conference on Machine Learning*, volume 162 of *Proceedings of Machine Learning Research*, pp. 4492–4519. PMLR, 17–23 Jul 2022. URL <https://proceedings.mlr.press/v162/cunningham22a.html>.
- Czyż, P., Grabowski, F., Vogt, J. E., Beerenwinkel, N., and Marx, A. Beyond normal: On the evaluation of mutual information estimators. In *Thirty-seventh Conference on Neural Information Processing Systems*, 2023. URL <https://openreview.net/forum?id=25vRtG56YH>.
- Czyż, P., Grabowski, F., Vogt, J. E., Beerenwinkel, N., and Marx, A. On the properties and estimation of pointwise mutual information profiles. *Transactions on Machine Learning Research*, 2025. ISSN 2835-8856. URL <https://openreview.net/forum?id=LdflD41Gn8>.
- De Bortoli, V., Liu, G.-H., Chen, T., Theodorou, E. A., and Nie, W. Augmented bridge matching. *arXiv preprint arXiv:2311.06978*, 2023.
- Dosi, G. and Roventini, A. More is different... and complex! the case for agent-based macroeconomics. *Journal of Evolutionary Economics*, 29:1–37, 2019.
- Duong, B. and Nguyen, T. Diffeomorphic information neural estimation. *Proceedings of the AAAI Conference on Artificial Intelligence*, 37(6): 7468–7475, Jun. 2023a. doi: 10.1609/aaai.v37i6.25908. URL <https://ojs.aaai.org/index.php/AAAI/article/view/25908>.
- Duong, B. and Nguyen, T. Normalizing flows for conditional independence testing. *Knowledge and Information Systems*, 66, 08 2023b. doi: 10.1007/s10115-023-01964-w.
- Fayad, A. and Ibrahim, M. On slicing optimality for mutual information. In *Thirty-seventh Conference on Neural Information Processing Systems*, 2023. URL <https://openreview.net/forum?id=JMuKfZx2xU>.
- Federici, M., Ruhe, D., and Forré, P. On the effectiveness of hybrid mutual information estimation, 2023. URL <https://arxiv.org/abs/2306.00608>.
- Franzese, G., BOUNOUA, M., and Michiardi, P. MINDE: Mutual information neural diffusion estimation. In *The Twelfth International Conference on Learning Representations*, 2024. URL <https://openreview.net/forum?id=0kWd8SJq8d>.
- Goldfeld, Z. and Greenewald, K. Sliced mutual information: A scalable measure of statistical dependence. In Beygelzimer, A., Dauphin, Y., Liang, P., and Vaughan, J. W. (eds.), *Advances in Neural Information Processing Systems*, 2021. URL <https://openreview.net/forum?id=SvrYl-FDq2>.
- Goldfeld, Z., van den Berg, E., Greenewald, K. H., Melnyk, I. V., Nguyen, N. H., Kingsbury, B., and Polyanskiy, Y. Estimating information flow in deep neural networks. In *ICML*, 2019.
- Goldfeld, Z., Greenewald, K., Niles-Weed, J., and Polyanskiy, Y. Convergence of smoothed empirical measures with applications to entropy estimation. *IEEE Transactions on Information Theory*, 66(7):4368–4391, 2020. doi: 10.1109/TIT.2020.2975480.
- Goldfeld, Z., Greenewald, K., Nuradha, T., and Reeves, G. Sliced mutual information: A quantitative study of scalability with dimension. In Oh, A. H., Agarwal, A., Belgrave, D., and Cho, K. (eds.), *Advances in Neural Information Processing Systems*, 2022. URL <https://openreview.net/forum?id=L-ceBdl2DPb>.
- Greenewald, K. H., Kingsbury, B., and Yu, Y. High-dimensional smoothed entropy estimation via dimensionality reduction. In *IEEE International Symposium on Information Theory, ISIT 2023, Taipei, Taiwan, June 25-30, 2023*, pp. 2613–2618. IEEE, 2023. doi: 10.1109/ISIT54713.2023.10206641. URL <https://doi.org/10.1109/ISIT54713.2023.10206641>.
- Gushchin, N., Kolesov, A., Korotin, A., Vetrov, D., and Burnaev, E. Entropic neural optimal transport via diffusion processes. In *Advances in Neural Information Processing Systems*, 2023.

- Gushchin, N., Kholkin, S., Burnaev, E., and Korotin, A. Light and optimal schrödinger bridge matching. In *Forty-first International Conference on Machine Learning*, 2024a.
- Gushchin, N., Selikhanovych, D., Kholkin, S., Burnaev, E., and Korotin, A. Adversarial schrödinger bridge matching. *arXiv preprint arXiv:2405.14449*, 2024b.
- Hjelm, R. D., Fedorov, A., Lavoie-Marchildon, S., Grewal, K., Bachman, P., Trischler, A., and Bengio, Y. Learning deep representations by mutual information estimation and maximization. In *International Conference on Learning Representations*, 2019. URL <https://openreview.net/forum?id=Bklr3j0cKX>.
- Ho, J. and Salimans, T. Classifier-free diffusion guidance. In *NeurIPS 2021 Workshop on Deep Generative Models and Downstream Applications*, 2021.
- Ho, J., Jain, A., and Abbeel, P. Denoising diffusion probabilistic models. *Advances in Neural Information Processing Systems*, 33:6840–6851, 2020.
- Huang, J., Jiao, Y., Kang, L., Liao, X., Liu, J., and Liu, Y. Schrödinger-föllmer sampler. *IEEE Transactions on Information Theory*, 2024.
- Ibe, O. *Markov processes for stochastic modeling*. Newnes, 2013.
- Igashov, I., Schneuing, A., Segler, M., Bronstein, M. M., and Correia, B. Retrobridge: Modeling retrosynthesis with markov bridges. In *The Twelfth International Conference on Learning Representations*, 2024.
- Kappen, B. Lecture notes in cds machine learning, September 2024.
- Kim, B., Hsieh, Y.-G., Klein, M., Cuturi, M., Ye, J. C., Kawar, B., and Thornton, J. Simple reflow: Improved techniques for fast flow models. In *The Thirteenth International Conference on Learning Representations*, 2025. URL <https://openreview.net/forum?id=fpvgSDKXGY>.
- Kingma, D. P. and Ba, J. Adam: A method for stochastic optimization, 2017.
- Kingma, D. P. and Dhariwal, P. Glow: Generative flow with invertible 1x1 convolutions. *Advances in neural information processing systems*, 31, 2018.
- Kloeden, P. E. *Numerical solution of stochastic differential equations / Peter E. Kloeden, Eckhard Platen*. Applications of mathematics; v. 23. Springer, Berlin, 1992. ISBN 0387540628.
- Kozachenko, L. F. and Leonenko, N. N. Sample estimate of the entropy of a random vector. *Problems Inform. Transmission*, 23:95–101, 1987.
- Kraskov, A., Stögbauer, H., and Grassberger, P. Estimating mutual information. *Phys. Rev. E*, 69:066138, Jun 2004. doi: 10.1103/PhysRevE.69.066138. URL <https://link.aps.org/doi/10.1103/PhysRevE.69.066138>.
- Léonard, C. A survey of the schrödinger problem and some of its connections with optimal transport. *arXiv preprint arXiv:1308.0215*, 2013.
- Léonard, C. Some properties of path measures. *Séminaire de Probabilités XLVI*, pp. 207–230, 2014.
- Léonard, C., Roelly, S., and Zambrini, J.-C. Reciprocal processes. a measure-theoretical point of view. *Probability Surveys*, 11:237–269, 2014.
- Linsker, R. Self-organization in a perceptual network. *Computer*, 21(3):105–117, 1988. doi: 10.1109/2.36.
- Liu, G.-H., Vahdat, A., Huang, D.-A., Theodorou, E. A., Nie, W., and Anandkumar, A. I²sb: Image-to-image schrödinger bridge. *arXiv preprint arXiv:2302.05872*, 2023.
- McAllester, D. and Stratos, K. Formal limitations on the measurement of mutual information. In Chiappa, S. and Calandra, R. (eds.), *Proceedings of the Twenty Third International Conference on Artificial Intelligence and Statistics*, volume 108 of *Proceedings of Machine Learning Research*, pp. 875–884. PMLR, 08 2020. URL <https://proceedings.mlr.press/v108/mcallester20a.html>.
- Nandwani, Y., Kumar, V., Raghu, D., Joshi, S., and Las-tras, L. A. Pointwise mutual information based metric and decoding strategy for faithful generation in document grounded dialogs. In *The 2023 Conference on Empirical Methods in Natural Language Processing*, 2023. URL <https://openreview.net/forum?id=NAmRjAIMkz>.
- Øksendal, B. *Stochastic differential equations*. Springer, 2003.
- Palmowski, Z. and Rolski, T. A technique for exponential change of measure for markov processes. *Bernoulli*, pp. 767–785, 2002.
- Peluchetti, S. Diffusion bridge mixture transports, schrödinger bridge problems and generative modeling. *Journal of Machine Learning Research*, 24(374):1–51, 2023.

- Polyanskiy, Y. and Wu, Y. *Information Theory: From Coding to Learning*. Cambridge University Press, 2024. ISBN 9781108832908. URL <https://books.google.ru/books?id=CySo0AEACAAJ>.
- Rhodes, B., Xu, K., and Gutmann, M. U. Telescoping density-ratio estimation. In Larochelle, H., Ranzato, M., Hadsell, R., Balcan, M., and Lin, H. (eds.), *Advances in Neural Information Processing Systems*, volume 33, pp. 4905–4916. Curran Associates, Inc., 2020. URL https://proceedings.neurips.cc/paper_files/paper/2020/file/33d3b157ddc0896addfb22fa2a519097-Paper.pdf.
- Rombach, R., Blattmann, A., Lorenz, D., Esser, P., and Ommer, B. High-resolution image synthesis with latent diffusion models. In *Proceedings of the IEEE/CVF Conference on Computer Vision and Pattern Recognition*, pp. 10684–10695, 2022.
- Ronneberger, O., Fischer, P., and Brox, T. U-net: Convolutional networks for biomedical image segmentation. In *Medical image computing and computer-assisted intervention—MICCAI 2015: 18th international conference, Munich, Germany, October 5-9, 2015, proceedings, part III 18*, pp. 234–241. Springer, 2015.
- Runge, J., Bathiany, S., Bollt, E., Camps-Valls, G., Coumou, D., Deyle, E., Glymour, C., Kretschmer, M., Mahecha, M. D., Muñoz-Marí, J., et al. Inferring causation from time series in earth system sciences. *Nature communications*, 10(1):2553, 2019.
- Schrödinger, E. Sur la théorie relativiste de l’électron et l’interprétation de la mécanique quantique. In *Annales de l’institut Henri Poincaré*, volume 2, pp. 269–310, 1932.
- Sen, R., Suresh, A. T., Shanmugam, K., Dimakis, A. G., and Shakkottai, S. Model-powered conditional independence test. In Guyon, I., Luxburg, U. V., Bengio, S., Wallach, H., Fergus, R., Vishwanathan, S., and Garnett, R. (eds.), *Advances in Neural Information Processing Systems*, volume 30. Curran Associates, Inc., 2017. URL https://proceedings.neurips.cc/paper_files/paper/2017/file/02f039058bd48307e6f653a2005c9dd2-Paper.pdf.
- Shi, Y., Bortoli, V. D., Campbell, A., and Doucet, A. Diffusion schrödinger bridge matching. In *Thirty-seventh Conference on Neural Information Processing Systems*, 2023. URL <https://openreview.net/forum?id=qy07OHsJT5>.
- Somnath, V. R., Pariset, M., Hsieh, Y.-P., Martinez, M. R., Krause, A., and Bunne, C. Aligned diffusion schrödinger bridges. In *Uncertainty in Artificial Intelligence*, pp. 1985–1995. PMLR, 2023.
- Song, J. and Ermon, S. Understanding the limitations of variational mutual information estimators. In *International Conference on Learning Representations*, 2020. URL <https://openreview.net/forum?id=B1x62TntDS>.
- Song, Y., Sohl-Dickstein, J., Kingma, D. P., Kumar, A., Ermon, S., and Poole, B. Score-based generative modeling through stochastic differential equations. In *International Conference on Learning Representations*, 2021.
- Steinke, T. and Zakyntinou, L. Reasoning About Generalization via Conditional Mutual Information. In Abernethy, J. and Agarwal, S. (eds.), *Proceedings of Thirty Third Conference on Learning Theory*, volume 125 of *Proceedings of Machine Learning Research*, pp. 3437–3452. PMLR, 09–12 Jul 2020. URL <https://proceedings.mlr.press/v125/steinke20a.html>.
- Stimper, V., Liu, D., Campbell, A., Berenz, V., Ryll, L., Schölkopf, B., and Hernández-Lobato, J. M. normflows: A pytorch package for normalizing flows. *Journal of Open Source Software*, 8(86):5361, 2023. doi: 10.21105/joss.05361. URL <https://doi.org/10.21105/joss.05361>.
- Stratos, K. Mutual information maximization for simple and accurate part-of-speech induction. In Burstein, J., Doran, C., and Solorio, T. (eds.), *Proceedings of the 2019 Conference of the North American Chapter of the Association for Computational Linguistics: Human Language Technologies, Volume 1 (Long and Short Papers)*, pp. 1095–1104, Minneapolis, Minnesota, June 2019. Association for Computational Linguistics. doi: 10.18653/v1/N19-1113. URL <https://aclanthology.org/N19-1113/>.
- Tishby, N. and Zaslavsky, N. Deep learning and the information bottleneck principle. *2015 IEEE Information Theory Workshop (ITW)*, pp. 1–5, 2015.
- Tong, A. Y., Malkin, N., Fatras, K., Atanackovic, L., Zhang, Y., Hugué, G., Wolf, G., and Bengio, Y. Simulation-free schrödinger bridges via score and flow matching. In *International Conference on Artificial Intelligence and Statistics*, pp. 1279–1287. PMLR, 2024.
- Tschannen, M., Djolonga, J., Rubenstein, P. K., Gelly, S., and Lucic, M. On mutual information maximization for representation learning. In *International Conference on Learning Representations*, 2020. URL <https://openreview.net/forum?id=rkxoh24FPH>.

- Tsur, D., Goldfeld, Z., and Greenewald, K. Max-sliced mutual information. In *Thirty-seventh Conference on Neural Information Processing Systems*, 2023. URL <https://openreview.net/forum?id=ce9B2x3zQa>.
- van den Oord, A., Li, Y., and Vinyals, O. Representation learning with contrastive predictive coding, 2019. URL <https://arxiv.org/abs/1807.03748>.
- Vargas, F., Thodoroff, P., Lamacraft, A., and Lawrence, N. Solving schrödinger bridges via maximum likelihood. *Entropy*, 23(9):1134, 2021.
- Vargas, F., Ovsianas, A., Fernandes, D., Girolami, M., Lawrence, N. D., and Nüsken, N. Bayesian learning via neural schrödinger–föllmer flows. *Statistics and Computing*, 33(1):3, 2023.
- Veličković, P., Fedus, W., Hamilton, W. L., Liò, P., Bengio, Y., and Hjelm, R. D. Deep graph infomax. In *International Conference on Learning Representations*, 2019. URL <https://openreview.net/forum?id=rklz9iAcKQ>.
- Wang, C., Franzese, G., Finamore, A., Gallo, M., and Michiardi, P. Information theoretic text-to-image alignment, 2024. URL <https://arxiv.org/abs/2405.20759>.
- Weglarczyk, S. Kernel density estimation and its application. *ITM Web of Conferences*, 23:00037, 01 2018. doi: 10.1051/itmconf/20182300037.
- Xu, A. and Raginsky, M. Information-theoretic analysis of generalization capability of learning algorithms. *Advances in neural information processing systems*, 30, 2017.
- Yang, H., Yao, J., Liu, W., Wang, Q., Qin, H., Kong, H., Tang, K., Xiong, J., Yu, C., Li, K., Xing, J., Chen, H., Zhuo, J., Fu, Q., Wei, Y., and Fu, H. Diverse policies recovering via pointwise mutual information weighted imitation learning, 2024. URL <https://arxiv.org/abs/2410.15910>.
- Yoon, E. B., Park, K., Kim, S., and Lim, S. Score-based generative models with lévy processes. *Advances in Neural Information Processing Systems*, 36:40694–40707, 2023.
- Zhou, L., Lou, A., Khanna, S., and Ermon, S. Denoising diffusion bridge models. In *The Twelfth International Conference on Learning Representations*, 2024.

A. Additional theoretical results

A.1. KL divergence estimator

In this section, we present a general result for the unbiased estimation of KL divergence between any two distributions $\pi_1(x), \pi_2(x) \in \mathcal{P}(\mathbb{R}^d)$ through the difference of drifts of the SDE formulation (4) of the reciprocal process induced by these distributions, i.e.:

$$Q_{\pi_1} = \int W_{|x_0, x_1}^\epsilon d\pi_1(x_1) dp(x_0), \quad (16)$$

$$Q_{\pi_2} = \int W_{|x_0, x_1}^\epsilon d\pi_2(x_1) dp(x_0). \quad (17)$$

Theorem A.1 (KL divergence decomposition). *Consider distributions $\pi_1(x), \pi_2(x), p(x) \in \mathcal{P}(\mathbb{R}^d)$ and reciprocal processes Q_{π_1}, Q_{π_2} induced by distributions $\pi_1(x), \pi_2(x)$ (16) (17). Then the KL divergence between distributions $\pi_1(x)$ and $\pi_2(x)$ can be represented in the following way:*

$$\text{KL}(\pi_1(x_1) \| \pi_2(x_1)) = \frac{1}{2\epsilon} \int_0^1 \mathbb{E}_{x_t \sim q_{\pi_1}(x_t, x_0)} [\|v^{\pi_1}(x_t, t, x_0) - v^{\pi_2}(x_t, t, x_0)\|_2^2] dt, \quad (18)$$

where

$$v^{\pi_1}(x_t, t, x_0) = \mathbb{E}_{x_1 \sim q_{\pi_1}(x_1 | x_t, x_0)} \left[\frac{x_1 - x_t}{1 - t} \right], \quad (19)$$

$$v^{\pi_2}(x_t, t, x_0) = \mathbb{E}_{x_1 \sim q_{\pi_2}(x_1 | x_t, x_0)} \left[\frac{x_1 - x_t}{1 - t} \right] \quad (20)$$

are the drifts of reciprocal processes Q_{π_1} and Q_{π_2} respectively. $p(x)$ can be any distribution of choice.

Our theorem allows us to estimate $\text{KL}(\pi_1(x) \| \pi_2(x))$ knowing only the drifts $v^{\pi_1}(x_t, t, x_0)$ and $v^{\pi_2}(x_t, t, x_0)$, which can be recovered using conditional bridge matching §2. Note that the expression (18) is very similar to the expression (12) in 4.1. However, there is a difference because (12) estimates the KL divergence between joint plans $\pi(x_0, x_1)$ and $\pi(x_0)\pi(x_1)$, where x_0, x_1 are random variables in the same dimension \mathbb{R}^d , but (18) estimates the KL divergence between general distributions that should not be represented as a joint plan between two random variables of the same dimension. Note that theorem A.1 holds for any distribution $p(x_0)$, which can be considered as part of the design space and optimised for each particular problem.

The KL divergence is a fundamental quantity, and its estimator can have many applications, such as mutual information estimation or entropy estimation using results described in Appendix A.2.

Proof. Consider

$$\begin{aligned} \text{KL}(\pi_1(x_1)p(x_0) \| \pi_2(x_1)p(x_0)) &= \underbrace{\text{KL}(p(x_0) \| p(x_0))}_{=0} + \mathbb{E}_{x_0} [\text{KL}(\pi_1(x_1|x_0) \| \pi_2(x_1|x_0))] = \\ &= \mathbb{E}_{x_0} [\text{KL}(\pi_1(x_1) \| \pi_2(x_1))] = \text{KL}(\pi_1(x_1) \| \pi_2(x_1)), \end{aligned}$$

Next to get

$$\text{KL}(\pi_1(x_1)p(x_0) \| \pi_2(x_1)p(x_0)) = \frac{1}{2\epsilon} \int_0^1 \mathbb{E}_{x_t \sim q_{\pi_1}(x_t, x_0)} [\|v^{\pi_1}(x_t, t, x_0) - v^{\pi_2}(x_t, t, x_0)\|_2^2] dt,$$

one can repeat all the steps that were taken to show:

$$\text{KL}(\pi(x_0, x_1) \|\pi(x_0)\pi(x_1)) = \frac{1}{2\epsilon} \int_0^1 \mathbb{E}_{q_\pi(x_t, x_0)} [\|v_{\text{joint}}(x_t, t, x_0) - v_{\text{ind}}(x_t, t, x_0)\|_2^2] dt,$$

in the proof of Theorem 4.1.

□

A.2. Differential entropy estimator

A general result on the information projections and maximum-entropy distributions suggests a way of calculating differential entropy through the KL divergence estimation. Consider the following theorem:

Theorem A.2 (Theorem 6.7 in (Kappen, 2024)). *Let $\phi: \mathbb{R}^n \rightarrow \mathbb{R}^k$ be any measurable function, an absolutely continuous probability distribution $p(x) \in \mathcal{P}(\mathbb{R}^d)$ and define $\alpha \stackrel{\text{def}}{=} \mathbb{E}_p \phi(x)$. Now, for any $\theta \in \mathbb{R}^k$ consider an absolutely continuous probability distribution $q_\theta \in \mathcal{P}(\mathbb{R}^d)$ with such probability density:*

$$q_\theta(x) = \exp(\langle \theta, \phi(x) \rangle - A(\theta)), \quad A(\theta) = \log \mathbb{E}_{q_\theta} e^{\langle \theta, \phi(x) \rangle}.$$

If there exists θ^* such that p is absolutely continuous w.r.t. q_{θ^*} and $\mathbb{E}_{q_{\theta^*}} \phi(x) = \alpha$, then

$$H(p) = H(q_{\theta^*}) - \text{KL}(p \| q_{\theta^*}),$$

Corollary A.3. *Let X be a d -dimensional absolutely continuous random vector with probability density function p , mean m and covariance matrix Σ . Then*

$$H(p) = H(\mathcal{N}(m, \Sigma)) - \text{KL}(p \| \mathcal{N}(m, \Sigma)), \quad H(\mathcal{N}(m, \Sigma)) = \frac{1}{2} \log((2\pi e)^d \det \Sigma),$$

where $\mathcal{N}(m, \Sigma)$ is a Gaussian distribution of mean m and covariance matrix Σ .

Corollary A.4. *Let X be an absolutely continuous random vector with probability density function p and $\text{supp } X \subseteq S$, where S has finite and non-zero Lebesgue measure $\mu(S)$. Then*

$$H(p) = H(\text{U}(S)) - \text{KL}(p \| \text{U}(S)), \quad H(\text{U}(S)) = \log \mu(S),$$

where $\text{U}(S)$ is a uniform distribution on S .

Similar results can also be obtained for other members of the exponential family. The first result (Corollary A.3) can be considered as a general recipe, while the second one (Corollary A.4) can be useful when we have prior knowledge about the support of X being restricted. Approach described in Theorem A.2 is very flexible and can be considered as a generalization of the method used in (Franzese et al., 2024).

In practice, to estimate the entropy of some probability distribution, it is sufficient to follow the one of the described in Corollaries A.3 and A.4 results. For example, if one uses Corollary A.3: 1) estimate mean m and covariance matrix Σ using a set of data samples, 2) calculate entropy $H(\mathcal{N}(m, \Sigma))$ via the provided closed form expression, 3) calculate the KL divergence $\text{KL}(p \| \mathcal{N}(m, \Sigma))$ via learning two conditional diffusion bridges models and utilizing our estimator ((18) from Theorem A.1).

A.3. Pointwise mutual information estimation

Mutual information can also be defined as an expectation of the *pointwise mutual information (PMI)*:

$$\text{PMI}_{X_0, X_1}(x_0, x_1) = \log \left[\frac{\pi(x_0, x_1)}{\pi(x_0)\pi(x_1)} \right] = \log \left[\frac{\pi(x_0 | x_1)}{\pi(x_0)} \right], \quad I(X_0; X_1) = \mathbb{E}_{x_0, x_1 \sim \pi(x_0, x_1)} \text{PMI}_{X_0, X_1}(x_0, x_1) \quad (21)$$

PMI quantifies local statistical interactions and is widely used in generative models alignment (Nandwani et al., 2023; Wang et al., 2024), reinforcement learning (Baram et al., 2021; Yang et al., 2024), and non-linear principal component analysis (Cunningham et al., 2022; Butakov et al., 2024a).

Next we present a way to estimate PMI using our framework of reciprocal processes and diffusions. Consider two distributions $\pi_1(x), \pi_2(x) \in \mathcal{P}(\mathbb{R}^d)$ and corresponding reciprocal processes Q_{π_1}, Q_{π_2} induced by distributions $\pi_1(x), \pi_2(x)$, respectively, i.e., (16) (17). Then the Radom-Nikodym derivative of these processes Q_{π_1} and Q_{π_2} can be decomposed by applying the disintegration theorem (Léonard, 2014):

$$\frac{dQ_{\pi}}{dQ_{\pi}^{\text{ind}}}(\{x_t\}_{t \in [0,1]}) = \frac{\pi(x_0, x_1)}{\pi(x_0)\pi(x_1)} \frac{dQ_{\pi|x_0, x_1}}{dQ_{\pi|x_0, x_1}^{\text{ind}}}(\{x_t\}_{t \in (0,1)}).$$

Next one can notice that Q_{π} and Q_{π}^{ind} are reciprocal processes. Therefore, their insides are identical Brownian Bridges, i.e., $Q_{\pi|x_0, x_1} = Q_{\pi|x_0, x_1}^{\text{ind}} = W_{|x_0, x_1}^{\epsilon}$, and their Radon-Nikodym derivative is equal to 1, i.e., $\frac{dQ_{\pi|x_0, x_1}}{dQ_{\pi|x_0, x_1}^{\text{ind}}}(\{x_t\}_{t \neq 0,1}) = 1$. Then one can take the additional expectation on the Brownian Bridge trajectories, i.e., $\{x_t\}_{t \neq 0,1}$, which are conditioned to start and end at points x_0 and x_1 , respectively:

$$\mathbb{E}_{\{x_t\}_{t \neq 0,1}} \left[\frac{dQ_{\pi}}{dQ_{\pi}^{\text{ind}}}(\{x_t\}) \right] = \mathbb{E}_{\{x_t\}_{t \neq 0,1}} \left[\frac{\pi(x_0, x_1)}{\pi(x_0)\pi(x_1)} \right] = \frac{\pi(x_0, x_1)}{\pi(x_0)\pi(x_1)}.$$

Finally by applying the Girsanov theorem (Øksendal, 2003) to the left side one can get:

$$\text{PMI}_{X_0, X_1}(x_0, x_1) = \frac{1}{2\epsilon} \int_0^1 \mathbb{E}_{q_{\pi}(x_t|x_0, x_1)} \|v_{\text{joint}}(x_t, t, x_0) - v_{\text{ind}}(x_t, t, x_0)\|^2 dt, \quad (22)$$

where v_{joint} and v_{ind} follow the same expression as in Theorem 4.1, i.e., (13) (14).

One can notice that this formula is very similar to the (12) but without conditioning on x_0, x_1 . Therefore, once having proper approximations of v_{joint} and v_{ind} , it is trivial to apply this result for the PMI estimation in practice by considering a slightly altered version of Algorithm 1.

A.4. Interaction information

Here we propose the generalization of *InfoBridge* for the *interaction information* estimation, which is the generalization of mutual information for more than two random variables. Interaction information for random variables X_0, X_1, X_2 is defined by:

$$\begin{aligned} I(X_0; X_1; X_2) &\stackrel{\text{def}}{=} I(X_0; X_1) - I(X_0; X_1|X_2) = \\ &= \text{KL}(\Pi(X_0, X_1) \parallel \Pi(X_0) \otimes \Pi(X_1)) - \text{KL}(\Pi(X_0, X_1|X_2) \parallel \Pi(X_0|X_2) \otimes \Pi(X_1|X_2)). \end{aligned} \quad (23)$$

This definition can be generalized for more random variables in a similar way. Both MI information terms can be estimated using Theorem 4.1 and practical algorithm *InfoBridge*. Applications of interaction information include neuroscience (Bounoua et al., 2024b), climate models (Runge et al., 2019), econometrics (Dosi & Roventini, 2019).

B. Experimental supplementary

In this section, additional experimental results and experimental details are described.

B.1. Low-dimensional benchmark

Additional results. In the Table 4 we present the results of low-dimensional benchmark (Czyż et al., 2023) with precision of 0.01 nats.

Dim	Filters	Time Embed	Parameters
≤ 5	64	64	43K
25	128	128	176K
50	256	256	699K

Table 2: Neural networks hyperparameters for low-dimensional (Czyż et al., 2023) benchmark. “Dim” - dimensionality of a MI estimation problem, “Filters” – number of filters in MLP, “Time Embed” – number filters in time embedding module, “Parameters” – number of overall neural networks parameters.

Experimental details. The benchmark implementation was taken from the official github repository:

<https://github.com/cbg-ethz/bmi>

Neural networks were taken of almost the same architecture as in (Franzese et al., 2024), which is MLP with residual connections and time embedding. Additional input s described in § 4.3 was processed the same way as time input. Number of parameters was taken depending on a dimensionality of the problem, see Table 2. Exponential Moving Average as a widely recognized training stabilization method was used with decay parameter of 0.999. For all the problems neural networks were trained during 100k iterations with $\epsilon = 1$, batch size 512, lr 0.0003. Mutual Information was estimated by Algorithm 1 with N pairs of samples $\{x_t^i, x_0^i, t^i\}_{i=1}^N$, where N is equal to the number of test samples times 10, i.e., 100k.

B.2. Image data benchmark

Experimental details for InfoBridge. The implementation of (Butakov et al., 2024a) image data benchmark was taken from the official github repository:

<https://github.com/VanessB/mutinfo>

Following authors of the benchmark, *gaussian* images were generated with all the default settings, *rectangle* images were generated with all the default settings, but minimum size of rectangle is 0.2 to avoid singularities. All the covariance matrices for the distributions defining the mutual information in the benchmark were generated without randomization of component-wise mutual information, but with randomization of the off-diagonal blocks of the covariance matrix.

To approximate the drift coefficient of diffusion U-Net (Ronneberger et al., 2015) with time, condition neural networks were used, special input s was processed as time input. For all the tests, neural networks were the same and had 2 residual layers per U-net block with 256 base channels, positional timestep encoding, upscale and downscale blocks consisting of two resnet blocks, one with attention and one without attention. The number of parameters is $\sim 27M$. During the training, 100k gradient steps were made with batch size of 64 and learning rate 0.0001. Exponential moving average was used with decay rate 0.999. Mutual Information was estimated by Algorithm 1 with N pairs of samples $\{x_t^i, x_0^i, t^i\}_{i=1}^N$, where N is equal to the number of test samples, i.e., 10k. Nvidia A100 was used for the InfoBridge training. Each run (one seed) took around 6 and 18 GPU-hours for the 16×16 and 32×32 image resolution setups, respectively.

Experimental details for other methods. In this part, we provide additional experimental details regarding other methods featured in Figure 1. We report the NN architectures used for neural estimators in Table 3.

MIENF. This method is based on bi-gaussianization of the input data via a Cartesian product of learnable diffeomorphisms (Butakov et al., 2024a). Such approach allows for a closed-form expression to be employed to estimate the MI.

With only minor stability-increasing changes introduced, we adopt the Glow (Kingma & Dhariwal, 2018) flow network architecture from (Butakov et al., 2024a), which is also reported in Table 3 (“GLOW”). We used the `normflows` package (Stimper et al., 2023) to implement the model. Adam (Kingma & Ba, 2017) optimizer was used to train the network on 10^5 images with a batch size 512, and the learning rate decreasing from $5 \cdot 10^{-4}$ to 10^{-5} geometrically. For averaging, we used 3 different seeds. Nvidia A100 was used to train the flow models. Each run (one seed) took no longer than four GPU-hours to be completed.

KSG. Kraskov-Stögbauer-Grassberger (Kraskov et al., 2004) mutual information estimator is a well-known k -NN non-parametric method, which is very similar to unweighted Kozachenko-Leonenko estimator (Kozachenko & Leonenko, 1987).

Table 3: The NN architectures used to conduct the tests with synthetic images in Section 5.

NN	Architecture
GLOW, $16 \times 16 (32 \times 32)$ images	$\times 1$: 4 (5) splits, 2 GLOW blocks between splits, $\times 2$ in parallel 16 hidden channels in each block, leaky constant = 0.01
	$\times 1$: Orthogonal projection linear layer $\times 2$ in parallel
Autoencoder, $16 \times 16 (32 \times 32)$ images	$\times 1$: Conv2d(1, 4, ks=3), BatchNorm2d, LeakyReLU(0.2), MaxPool2d(2)
	$\times 1$: Conv2d(4, 8, ks=3), BatchNorm2d, LeakyReLU(0.2), MaxPool2d(2)
	$\times 2(3)$: Conv2d(8, 8, ks=3), BatchNorm2d, LeakyReLU(0.2), MaxPool2d(2)
	$\times 1$: Dense(8, dim), Tanh, Dense(dim, 8), LeakyReLU(0.2)
	$\times 3(4)$: Upsample(2), Conv2d(8, 8, ks=3), BatchNorm2d, LeakyReLU(0.2)
Critic NN, $16 \times 16 (32 \times 32)$ images	$\times 1$: Upsample(2), Conv2d(8, 4, ks=3), BatchNorm2d, LeakyReLU(0.2)
	$\times 1$: Conv2d(4, 1, ks=3), BatchNorm2d, LeakyReLU(0.2)
	$\times 1$: [Conv2d(1, 16, ks=3), MaxPool2d(2), LeakyReLU(0.01)] $\times 2$ in parallel
	$\times 1(2)$: [Conv2d(16, 16, ks=3), MaxPool2d(2), LeakyReLU(0.01)] $\times 2$ in parallel
	$\times 1$: Dense(256, 128), LeakyReLU(0.01)
	$\times 1$: Dense(128, 128), LeakyReLU(0.01)
	$\times 1$: Dense(128, 1)

This method employs distances to k -th nearest neighbors to approximate the pointwise mutual information, which is then averaged.

We used $k = 1$ (one nearest neighbour) for all the tests. The number of samples was 10^5 for Gaussian images and 10^4 for images of rectangles (we had to lower the sampling size due to degenerated performance of the metric tree-based k -NN search in this particular setup). A single core of AMD EPYC 7543 CPU was used for nearest neighbors search and MI calculation. Each run (one seed) took no longer than one CPU-hour to be completed.

AE+WKL 5-NN. The idea of leveraging lossy compression to tackle the curse of dimensionality and provide better MI estimates is well-explored in the literature (Goldfeld & Greenwald, 2021; Goldfeld et al., 2022; Tsur et al., 2023; Fayad & Ibrahim, 2023; Greenwald et al., 2023; Butakov et al., 2024b). In our work, we adopt the non-linear compression setup from (Butakov et al., 2024b), which employs autoencoders for data compression and weighted Kozachenko-Leonenko method (Berrett et al., 2019) for MI estimation in the latent space.

The autoencoders were trained using Adam optimizer on 10^5 images with a batch size 512, a learning rate 10^{-3} and MAE loss for 10^4 steps. For averaging, we used 5 different seeds. Nvidia A100 was used to train the autoencoder model. Each run (one seed) took no longer than one GPU-hour to be completed.

MINE, NWJ, InfoNCE. These discriminative approaches are fundamentally alike: each method estimates mutual information by maximizing the associated KL-divergence bound:

$$I(X; Y) = \text{KL}(\Pi_{X,Y} \parallel \Pi_X \otimes \Pi_Y) \geq \sup_{T: \mathcal{X} \times \mathcal{Y} \rightarrow \mathbb{R}} \mathbb{F}[T(x, y)], \quad (24)$$

where T is measurable, and \mathbb{F} is some method-specific functional. In practice, T is approximated via a neural network, with the right-hand-side in (24) being used as the loss function.

Motivated by this similarity, we use a nearly identical experimental framework to assess each approach within this category. To approximate T in experiments with synthetic images, we adopt the critic NN architecture from (Butakov et al., 2024a), which we also report in Table 3 (“Critic NN”).

The networks were trained via Adam optimizer on 10^5 images with a learning rate 10^{-3} , a batch size 512 (with InfoNCE being the only exception, for which we used batch size 256 for training and 512 for evaluation due to memory constraints), and MAE loss for 10^5 steps. For averaging, we used 5 different seeds. Nvidia A100 was used to train the models. In any setup, each run (one seed) took no longer than two GPU-hours to be completed.

B.3. Additional experiments with AE+WKL estimator using higher bottleneck dimensionality

Prior works suggest that non-parametric MI estimators are highly prone to the curse of dimensionality compared to NN-based approaches (Goldfeld et al., 2020; Czyż et al., 2023; Butakov et al., 2024a). In particular, Figures 2 and 3 in (Goldfeld et al., 2020) and Table 1 in (Butakov et al., 2024a) indicate that weighted Kozachenko-Leonenko estimator fails to yield reasonable estimates at all if the dimensionality reaches certain threshold. That is why autoencoders are used in our setup to acquire MI estimates for high-dimensional synthetic images.

However, this approach introduces a substantial inductive bias. Not only we assume the data to be distributed on a manifold, but also select the bottleneck dimensionality of the autoencoders to be equal to the ground-truth intrinsic dimensionality, which is usually not available in practical scenarios. Such prior knowledge allows for remarkable results, as it can be seen in Figure 1. However, we argue that even slight changes to this experimental protocol can lead to severe problems. In the Gaussian images setup, increasing the bottleneck dimensionality from 2 (which is the intrinsic dimensionality of the dataset in question) to 4 completely destabilizes the estimator. We report our results in Figure 3; all the other details of the experimental setup are identical to the settings used for Figure 1.

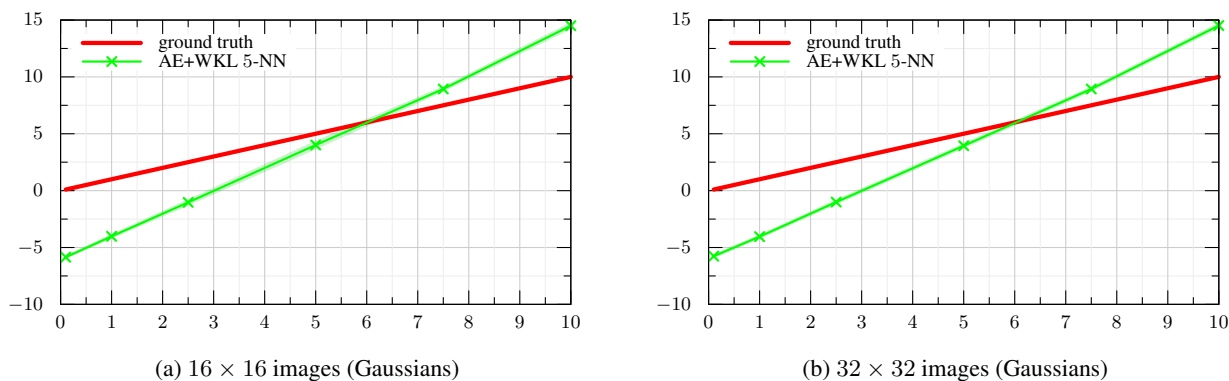


Figure 3: Results for AE+WKL 5-NN with increased bottleneck dimensionality. Along x axes is $I(X_0; X_1)$, along y axes is MI estimate $\hat{I}(X_0; X_1)$. We plot 99% asymptotic CIs acquired from different seed runs (5 seeds in total).

GT	0.22 0.43 0.29 0.45 0.41 0.41 0.41 1.02 1.02 1.02 1.02 0.96 0.98 0.29 1.01 1.28 0.99 0.41 0.99 0.58	1.62 0.41 1.02 1.02 1.02 1.02 1.02 1.02 1.02 1.02 1.02 1.02 1.02 1.02 1.02 1.02 1.02 1.02 1.02 1.02	0.22 0.43 0.19 0.29 0.18 0.45 0.30 0.41 1.71 0.33 0.41
InfoBridge	0.26 0.48 0.31 0.45 0.44 0.40 0.38 0.95 0.95 0.96 0.98 0.29 1.01 1.28 0.99 0.41 0.99 0.58	1.68 0.44 0.98	0.00 0.00 0.21 0.31 0.2 0.55 0.34 0.49 1.33 0.40 0.38
MINDE-f ($\sigma = 1$)	0.21 0.40 0.26 0.40 0.41 0.41 0.41 1.10 1.01 1.00 1.01 0.29 0.91 1.18 1.00 0.42 1.00 0.59	1.72 0.40 0.96 0.96 0.99 0.87 0.90 0.90 0.95 0.95 0.98	0.17 0.35 0.18 0.25 0.17 0.47 0.29 0.49 1.65 0.31 0.41
MINDE-f	0.22 0.42 0.28 0.42 0.41 0.42 0.42 1.19 1.02 1.02 1.02 0.29 0.99 1.31 1.02 0.41 1.01 0.59	1.73 0.41 1.07 0.99 0.99 0.95 0.92 0.93 1.07 0.99 0.98	0.13 0.24 0.20 0.30 0.18 0.48 0.31 0.40 1.67 0.31 0.42
MINDE-c ($\sigma = 1$)	0.21 0.42 0.27 0.42 0.41 0.41 0.41 0.96 1.00 0.99 1.01 0.29 1.00 1.26 1.01 0.41 1.01 0.59	1.62 0.40 0.94 0.97 0.95 0.92 0.94 0.93 0.93 0.96 0.94	0.13 0.28 0.18 0.29 0.18 0.42 0.30 0.32 1.67 0.31 0.41
MINDE-c	0.21 0.42 0.28 0.42 0.41 0.41 0.41 1.00 1.01 1.01 1.01 0.29 1.00 1.27 1.01 0.41 1.01 0.59	1.60 0.40 0.98 0.99 0.98 0.92 0.94 0.94 0.94 0.98 0.98	0.14 0.26 0.19 0.28 0.17 0.44 0.29 0.40 1.66 0.31 0.41
MINE	0.23 0.38 0.24 0.36 0.40 0.41 0.41 0.96 0.99 0.98 1.01 0.30 0.99 1.28 1.01 0.41 1.00 0.59	1.60 0.39 0.88 0.90 0.90 0.81 0.70 0.65 0.88 0.89 0.87	0.02 0.01 0.12 0.12 0.13 0.16 0.22 0.39 1.66 0.32 0.41
InfoNCE	0.22 0.41 0.27 0.40 0.41 0.41 0.41 0.98 1.01 1.01 1.02 0.29 0.99 1.28 1.01 0.41 1.02 0.59	1.61 0.40 0.92 0.98 0.99 0.83 0.84 0.82 0.92 0.96 0.96	0.15 0.30 0.18 0.27 0.17 0.41 0.28 0.40 1.69 0.32 0.41
D-V	0.22 0.41 0.27 0.40 0.41 0.41 0.41 0.98 1.01 1.01 1.02 0.29 0.99 1.28 1.01 0.41 1.02 0.59	1.61 0.40 0.93 0.98 0.99 0.82 0.82 0.81 0.92 0.96 0.96	0.01 0.05 0.11 0.13 0.15 0.22 0.21 0.40 1.69 0.32 0.41
NWJ	0.22 0.41 0.27 0.40 0.41 0.41 0.41 0.98 1.01 1.01 1.02 0.29 0.99 1.28 1.01 0.41 1.02 0.59	1.60 0.40 0.93 0.98 0.98 0.82 0.82 0.80 0.92 0.95 0.96	0.03 0.02 0.04 -0.65 0.12 0.21 0.21 0.40 1.69 0.32 0.41
KSG	0.22 0.38 0.19 0.24 0.42 0.42 0.42 0.17 0.87 0.66 1.03 0.29 0.20 1.07 0.95 0.41 0.74 0.57	1.28 0.42 0.20 0.92 0.72 0.18 0.71 0.55 0.20 0.90 0.69	0.16 0.22 0.09 0.12 0.07 0.20 0.15 0.42 1.68 0.32 0.42
LNN	0.25 0.89 2.71 6.65 0.41 0.42 0.42	2.49 7.27 3.10 7.31	0.39 2.38 7.24
CCA	0.00 0.00 0.00 0.00 0.34 0.41 0.38 0.99 0.95 0.96 1.02 0.29 1.06 1.33 1.02 0.41 1.02 0.60	1.75 0.39 1.00 0.97 0.96 0.86 0.23 0.39 0.99 0.84 0.90	0.33 0.95 0.11 0.13 0.01 0.31 0.02 0.02 1.63 0.19 0.38
DoE(Gaussian)	0.16 0.48 0.27 0.57 0.37 0.39 0.67 0.97 0.96 0.95 0.35 0.67 7.83 0.95 0.64 0.94 1.27 16.11	0.37 0.70 0.99 0.95 0.48 0.58 0.56 0.57 0.74 0.77	6.74 7.93 1.78 2.54 0.61 4.24 1.17 1.57 0.11 0.38
DoE(Logistic)	0.13 0.37 0.21 0.43 0.41 0.35 0.36 0.62 0.92 0.92 0.95 0.34 0.69 7.83 0.95 0.63 0.93 1.27 16.15	0.41 0.78 1.08 1.05 0.47 0.60 0.55 0.67 0.79 0.81	-0.32 2.00 0.46 0.82 0.29 1.48 0.59 1.58 0.08 0.35
dist			
			Wiggly @ Bivariate Nm 1 x 1
			Uniform 1 x 1 (additive noise=.75)
			Uniform 1 x 1 (additive noise=.1)
			Swiss roll 2 x 1
			St 5 x 5 (dof=3)
			St 5 x 5 (dof=2)
			St 3 x 3 (dof=3)
			St 3 x 3 (dof=2)
			St 2 x 2 (dof=2)
			St 2 x 2 (dof=1)
			St 1 x 1 (dof=1)
			Sp @ Nm CDF @ Mn 5 x 5 (2-pair)
			Sp @ Nm CDF @ Mn 3 x 3 (2-pair)
			Sp @ Nm CDF @ Mn 25 x 25 (2-pair)
			Sp @ Mn 5 x 5 (2-pair)
			Sp @ Mn 3 x 3 (2-pair)
			Sp @ Mn 25 x 25 (2-pair)
			Nm CDF @ Mn 5 x 5 (2-pair)
			Nm CDF @ Mn 3 x 3 (2-pair)
			Nm CDF @ Mn 25 x 25 (2-pair)
			Nm CDF @ Bivariate Nm 1 x 1
			Mn 50 x 50 (dense)
			Mn 5 x 5 (dense)
			Mn 5 x 5 (2-pair)
			Mn 3 x 3 (dense)
			Mn 3 x 3 (2-pair)
			Mn 25 x 25 (dense)
			Mn 25 x 25 (2-pair)
			Mn 2 x 2 (dense)
			Mn 2 x 2 (2-pair)
			Hc @ Mn 5 x 5 (2-pair)
			Hc @ Mn 3 x 3 (2-pair)
			Hc @ Mn 25 x 25 (2-pair)
			Hc @ Bivariate Nm 1 x 1
			Bivariate Nm 1 x 1
			Bimodal 1 x 1
			Asinh @ St 5 x 5 (dof=2)
			Asinh @ St 3 x 3 (dof=2)
			Asinh @ St 2 x 2 (dof=1)
			Asinh @ St 1 x 1 (dof=1)

Table 4: Mean estimate over 10 seeds using $10 \cdot 10^3$ test samples compared each against the ground-truth. Size of train dataset for every neural method is 100k. All the methods for comparison with InfoBridge were taken from (Franzese et al., 2024). List of abbreviations (*Mn*: Multinomial, *St*: Student-t, *Nm*: Normal, *Hc*: Half-cube, *Sp*: Spiral)